Babeș-Bolyai University Cluj-Napoca

Faculty of Environmental Science and Engineering

Multi-method luminescence dating studies using quartz and feldspars extracted from loess deposits in Europe, Asia and Oceania

- Doctoral Thesis Summary -

ANCA GIURGEA (AVRAM)

Promoters: Prof. Dr. Alida Gabor

Cluj-Napoca 2021

The research discussed in the present thesis was carried out at the Environmental Radioactivity and Nuclear Dating Centre, Interdisciplinary Research Institute on Bio-Nano-Science, Babeș-Bolyai University in Cluj-Napoca, Romania.

Anca Giurgea (Avram) benefited from financial support from:

- The Romanian National Authority for Scientific Research, PN-III-P3-3.6-H2020-2016-0015 contract number 7/2016.
- European Research Council (ERC) under the European Union's Horizon 2020 research and innovation program ERC-2015-StG (grant agreement No [678106]).
- EEA-RO-NO-2018-0126 contract nr. 3/2019 "Cave deposits as archives of climate and environmental changes. A Center of Excellence in speleological research".

Table of contents

Keywords: luminescence dating, optically stimulated luminescence (OSL) dating, cuartz, feldspars, SAR-OSL protocol, pIRIR protocols, fading measurements, residual doses, dose recovery test, natural and laboratory dose response curves, saturație characteristics, loess-paleosol sections.

1. Introduction

Providing accurate and precise chronologies for the timing of the climatic changes that have modelled the Earth evolution during the glacial-interglacial cycles is crucial and this is achieved by the analysis of archives that recorded these climatic oscillations.

The available archives for this purpose are cryogenic, marine or terrestrial. Loess-paleosol deposits represent valuable records of past climate change on continents. The simplified definition of loess is that of a terrestrial sediment dominated by silt, formed by dust which was entrained, transported and deposited by wind (**Pye 1987, 1995; Muhs 2007**). Loess deposits are largely distributed on both northern and southern hemispheres, covering around 10 % of the continental surface of the Earth (**Pye 1987**). When palaeosols are embedded within loess, then a loess-paleosol profile is found. The first application of luminescence for dating loess was carried out by **Wintle et al. in 1984**.

Optically Stimulated Luminescence (OSL) dating technique is an absolute chronological method that enables to assess the time elapsed since a material was last exposed to sunlight. The method uses minerals such as quartz or feldspars. Their crystalline structure and inherent natural defects results in their property to store the natural ionising radiation in the form of trapped charge. This charge is stored in the form of electrons captured in the electron traps and corresponding holes trapped at trapped hole centres. These can recombine upon stimulation with heat or light, recombination that can result in the emission of light. The luminescence dating method uses a luminescence signal that is optically sensitive. During light exposure of the mineral, the latent luminescence signal previously acquired is erased until it is completely removed. The removing process of the luminescence signal is also known as bleaching. Once the grain is no longer exposed to light, the luminescence signal starts to accumulate again due to the interaction of naturally occurring radioactivity with the mineral grain lattice. In order to obtain a luminescence age, the ratio between the total dose received since bleaching and the annual dose is determined. The annual dose is derived from the specific activities of the ^{238}U, ^{232}Th and ^{40}K by the application of conversion factors while the total dose is measured as an equivalent dose by a calibration procedure under laboratory conditions following measurement protocols that are developed particularly for quartz or feldspars. In the case of equivalent dose estimation, the single aliquot regenerative (SAR) OSL protocol (**Murray and Wintle 2000, 2003**) initially developed for quartz has revolutionised luminescence dating by increasing the precision and flexibility of measurements.

The protocol implies the readout of the natural OSL signal emitted by quartz by blue light stimulation and comparing this natural OSL signal with the luminescence signals obtained by the application of different known doses on the same aliquot. As an individual dose can be determined using a single aliquot, and many aliquots (usually more than 10) are analysed for each sample, the protocol allows determining equivalent doses for samples with a high level of precision, typical standard errors being less than 5% (**Murray and Olley 2002; Rhodes et al., 2003**). Over the past two decades, the SAR-OSL protocol has been tested and applied on quartz of different grain sizes (fine (4-11 μm) quartz grains and coarse (63-90, 90-125, 125-180, 180-250 μm) quartz grains) from a large variety of sediments (e.g**., Stevens et al., 2006; Lu et al., 2007; Lai, 2010; Buylaert et al., 2008; Timar-Gabor et al., 2011; Constantin et al., 2012, 2014; Veres et al., 2018; Perić et al., 2019; Tecsa et al., 2020a, b; Groza et al., 2020**). Regardless of the quartz grain size used numerous studies have reported age underestimation for samples that are older than 70 ka (corresponding to an equivalent dose of >~ 100-200 Gy) (e.g**., Watanuki et al., 2003; Murray et al., 2007; Buylaert et al., 2007; Timar et al., 2010; Lai 2010; Lowic et al., 2010**). **Timar-Gabor et al. (2011)** further confirmed this, but also showed for the first time that an age deviation exists between fine quartz ages and coarse quartz ages for loess in Romania.

Subsequent studies on different regions (e.g., **Constantin et al., 2014; Timar-Gabor et al., 2012, 2015a, 2017; Timar-Gabor and Wintle, 2013**) have showed that this phenomenon is not an isolated one. The underestimation of fine quartz ages is more severe and displays an earlier onset (e.g., **Timar-Gabor et al., 2011, 2012; Timar-Gabor and Wintle., 2013**). The age discrepancy cannot be attributed to issues related to annual dose estimation as higher equivalent doses were obtained for coarse (63-90 μm) quartz grains compared to fine (4-11 μm) quartz grains, and one would expect an opposite trend based on dosimetric considerations.

The dose response curves of quartz do not follow a single saturating exponential dependency that would be expected based on simple models and were shown to be well represented by a sum of two saturating exponential functions (e.g., **Murray et al., 2007, Pawley et al., 2010, Timar-Gabor et al., 2012**). The saturation characteristics of fine and coarse quartz fraction were investigated (**Constantin et al., 2012; Timar-Gabor et al., 2012, 2015b**) and it was found that the dose response curves overlap up to ~100-200 Gy while for higher doses the curves diverge. A wide range of quartz fractions were investigated in this context (**Timar-Gabor et al., 2017**) and the results showed that the saturation characteristics and the diameter of the grains follows an inverse square roots relationship (**Timar-Gabor et al., 2017**).

The discrepancy between the equivalent doses is thought to reside in the differences observed between the natural and laboratory dose response curves for both fine and coarse quartz (**Chapot et al., 2012; Timar-Gabor and Wintle 2013; Avram et al., 2020**).

Since based on natural and laboratory dose response curve comparison the upper dating limit of quartz is restricted to an age of ~50 ka to ~100 ka for quartz, an extension of the datable age range is desirable. Therefore, alternative natural luminescence dosimeters were investigated in this purpose. Feldspars are considered a substitute of quartz due to some of their advantages: (1) unlike quartz, feldspars are sensitive to IR stimulation and (2) it was reported that the luminescence signals emitted by feldspars continues to grow at higher doses than quartz, thus extending the dose range over which luminescence ages can be obtained. However, the use of feldspars has been hampered by the phenomenon of anomalous fading, a loss of signal due to quantum mechanical tunnelling of charge (**Wintle 1973; Spooner 1992, 1994**). Recent advances have been made in the attempt to circumvent fading, since **Thomsen et al. (2008)** measured lower fading rates for the infrared stimulated luminescence (IRSL) signal measured at a temperature of 225 ^{0}C after the IR stimulation at 50 ^{0}C. Two elevated temperature post infrared-infrared (pIRIR) protocols based on SAR procedure have been developed to reduce the signal which is susceptible to fading. The most used and tested pIRIR protocols are $pIRIR_{225}$ (**Roberts 2008; Buylaert et al., 2009; Wacha and Frechen 2011**) and $pIRIR_{290}$ (**Buylaert et al., 2011a, 2012; Thiel et al., 2011a**).

Despite the higher stability of the pIR-IRSL signals at higher temperature than the IRSL signal stimulated at 50 ^{0}C, their bleachability is also considered an issue (**Thomsen et al., 2008; Buylaert et al., 2009; Thiel et al., 2011a**). Previous studies reported residual doses of a few Grays even after prolongued exposure to sunlight or to the solar simulator (e.g., **Buylaert et al., 2011b**, **2012; Murray et al., 2012; Thiel et al., 2011a; Steven et al., 2011**).

Another controversial issue reported for pIRIR protocols are the dose recovery test results. The dose recovery test is used to assess the accuracy of a SAR procedure for measuring a known laboratory given dose. This dose is given to a sample that has its signal reset and is measured as an unknown dose. The dose recovery ratio is then quantified by dividing the obtained result to the given dose and should be ideally equal to one. Even though various studies reported good dose recovery ratios on feldspars extracted from different loess deposits over the world (e.g. **Buylaert et al., 2011a, Thiel et al., 2012; Sohbati et al., 2016; Yi et al., 2016, 2018; Bösken et al., 2017; Stevens et al., 2018),** there are some other studies report

evidence of poor dose recovery ratios (e.g. **Stevens et al., 2011; Thiel et al., 2011b; Murray et al., 2014; Y. Li et al., 2018; Veres et al., 2018; Avram et al., 2020)**.

Since each protocol has its advantages and limitations as presented in the aforementioned text, the objectives of this thesis are: (i) to evaluate the applicability of each protocol (SAR-OSL, $pIRIR_{225}$ and $pIRIR_{290}$) on quartz and polymineral fine grains extracted from the same samples; (ii) to assess the dose range over which each protocol can measure reliable equivalent doses and thus over which time interval reliable ages for quartz and polymineral fine grains can be obtained; (iii) to explore the polymineral fine grains bleachability when $pIRIR_{225}$ and $pIRIR_{290}$ protocols are used; (iv) to check if both $pIRIR_{225}$ and $pIRIR_{290}$ protocols are a satisfying solution for circumventing the fading issue and (v) to assess the influence of the test dose magnitude on the dose recovery ratios of pIRIR protocols. To achieve these goals loess samples of various ages collected over three continents have been investigated in the framework of the research project "Integrated dating approach for terrestrial records of past climate using trapped charge methods" INTERTRAP (StG 678106, HORIZON 2020) funded by the European Research Council (ERC).

2. Basic concept of Optically Stimulated Luminescence dating and Measurements Protocols

2.1 Principles of OSL dating

Luminescence dating represents a geochronological technique that can provide numerical dates of past events. This method has the advantage of using minerals such as quartz and feldspars which are found ubiquitous in the Earth's crust.

Luminescence phenomena refer to the light emitted by minerals as a response to an external stimulation source that leads to a transition from a metastable state to equilibrium. "Optical stimulated luminescence" is the term used when the stimulation is either by visible light (Optically Stimulated Luminescence OSL) or near-infrared radiation (Infrared Stimulated Luminescence, IRSL). The moment which is dated represent the last exposure to sunlight of the mineral grains when the latent luminescence signal that was previously acquired due to ionising radiation from the natural occurring radioactivity is removed by light. This process of resetting the signals is known as bleaching. In the case of sediments, the moment that is dated by OSL coincides with the time of deposition. A schematic representation of the principles of luminescence dating is presented in **Figure 2.1.**

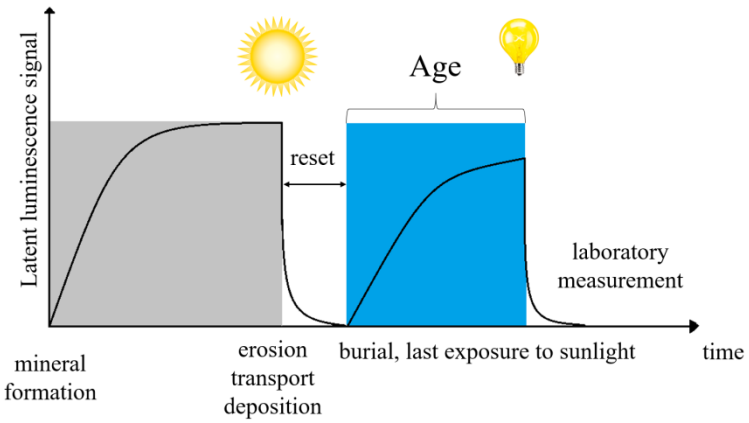

Figure 2.1 Schematic representation of the optically stimulated luminescence dating principles in the case of sedimentary environments

The luminescence age (i.e., the period of time since the minerals were last exposed to sunlight) is determined by using the following formula:

$$\text{Age (ka)} = \frac{Equialent\ Dose\ (Gy)}{\text{Annual Dose } (\frac{\text{Gy}}{\text{ka}})} \qquad \text{Eq. (2.1)}$$

where the Equivalent dose (Gy) represents the dose absorbed by the mineral during burial and the annual dose (Gy a^{-1} or Gy ka^{-1}) expresses the absorption rate of energy by the mineral grains per unit of mass during a certain period of time.

The single aliquot regenerative dose (SAR) protocol (**Murray and Wintle 2000, 2003**) was developed and applied worldwide on quartz in order to measure the De while for feldspars were developed measurement protocols based on the SAR procedure that use a double infrared stimulation, namely $pIRIR_{225}$ and $pIRIR_{290}$.

Beside the equivalent dose, the annual dose has to be determined for obtaining the age. The annual dose is derived from the radionuclide concentration of ^{238}U, ^{232}Th and ^{40}K which are measured by using high-resolution gamma spectrometry.

2.2 Mechanism of Optically Stimulated Luminescence

The OSL mechanism for materials such as insulator and semi-conductors can be described in term of energy band model. Therefore, in a crystalline structure the valence and the conduction band are separated by a forbidden band (gap band) where no energy levels are allowed. Since the crystalline structure of the natural minerals is not perfect, the defects will give rise to metastable energy levels located within the band gap. When the mineral interacts with ionising radiation, the electrons from the valence band may gain sufficient energy to shift to the conduction band. For each electron that was shifted, a hole is created in the valence band. For most charge, the excitation energy is lost and they are relocated in the valence band. Another possibility is that excited electrons to get trapped in the defect centres within the forbidden gap. The same process is applicable to holes. When the system is exposed to thermal or optical stimulation, the trapped electrons may receive sufficient energy to return to the conduction band. Once released, they can be trapped again or they can recombine with holes in the recombination centres. As a result of the recombination, phonons or light (radiative recombination) can occur. Radiative recombination takes place in the luminescence centres. The preceding description is the simplest version of the luminescence mechanism which implies only one trap and one recombination centre. This model is known as the general one trap model.

2.3 Minerals and signals used for dating

2.3.1 Quartz

Quartz is one of the most common minerals in the Earth's continental crust. It can be found in volcanic rocks, granite, hydrothermal veins, as well as in sedimentary rocks. Quartz crystals are formed in different temperature and pressure

conditions, depending on the environment they occur. The molecular structure of quartz consists of almost 100% SiO_2. The chemical bond between Si and O atoms has ionic (40%) and covalent (60%) nature.

2.3.2 The energy band model for quartz

The crystal structure of natural quartz implies the presence of more than one trap and a recombination centre. It has been shown that quartz OSL signal comprises three different components fast, medium and slow (Smith and Rhodes, 1994; Bailey et al., 1997). One of the most used energy band models for quartz is that developed by **Bailey (2001)**. Based on this model, further improvements were added by **Bailey (2002, 2004)** and **Pagonis et al. (2007, 2008)** with regard of more specific aspects. The energy band model presented by **Bailey (2001)** includes five electron trapping centres localised at different depths below the conduction band and four recombination centres in the proximity of the valence band.

2.3.3 Feldspars

Feldspar minerals refer to an aluminosilicate's group and are considered the most abundant minerals from the continental crust of the Earth. Their chemical composition consists of a three-dimensional structure where the oxygen atoms from AlO_4 and SiO_4 tetrahedral units are shared. Their chemical composition allows charge compensating cations to occupy large interstices within the tetrahedral framework and create a group of feldspars with different chemical combinations (**Bøtter-Jansen et al., 2003**). The principal substitutional elements are sodium (Na^+), potassium (K^+) and calcium (Ca^{2+}). Based on their chemical composition, two groups of feldspars can be recognized: (a) alkali-feldspars refer to the group where potassium or sodium atoms bearing feldspars, and (b) plagioclases, representing the feldspar group with sodium and calcium bearing members (**Baril, 2002**)

2.3.4 The energy band model for feldspars

The most recent model for luminescence mechanism in feldspars was proposed by **Jain and Ankjaergaard (2011).** This model involves a single dosimetric trap and asserts the importance of the band-tail states in describing the luminescence process. They suggested that stimulation photon energy influences the routes for the charge transport. The model of luminescence production in feldspars proposed by Jain and Ankjaergaard (2011) can be summarized in a two-step process: (a) the electrons captured in the dosimetric IRSL trap are shifted to its excited state, (b) electrons in the excited state diffuse out to the band tail states or into the conduction band. The origin of the post IR IRSL signal proposed by **Jain and Ankjaergaard (2011)** can be described as a two-step process. In the first step, the excited electrons

recombine with holes in the proximal recombination as a result of the first IR stimulation. A subsequent IR stimulation at elevated temperature is capable to access distant holes through the high energy band tail states. Since the first IR stimulation removed the most proximal pairs, the post IR-IRSL signal is the result of the distant electron-hole recombination which make it less susceptible to tunnelling from the ground state. The signal stability has been also demonstrated by **Thomsen et al. (2008)** and **Buylaert et al. (2009)**. The model predicts that the stability of the post IR IRSL signal is directly dependent of the stimulation temperature.

2.4 Anomalous fading

The athermal loss of the luminescence signal is known in literature as anomalous fading (**Wintle, 1973**) and was observed ubiquitous in sedimentary feldspars from various regions of the world (**Huntley and Lamothe, 2001; Huntley and Lian, 2006**). From the luminescence point of view, this signal loss will lead to age underestimation.

Quantum mechanical tunnelling was the commonly accepted explanation for anomalous fading.

In order to correct the underestimated ages affected by anomalous fading, several methods have been developed. **Huntley and Lamothe (2001)** divided the fading correction methods into three categories: circumvention, variability and correction.

Circumvention implies the use of a signal that does not display any signal loss. Thermal treatments, storage and/or exposure to low energy photons have been tried in order to remove the component susceptible to fading. Other applications suggested the use of deeper traps or a long-term stability luminescence emission.

Correction methods were developed based on the idea that if the fading rates can be measured in laboratory than the age correction should be possible (e.g. Huntley and Lamothe 2001; Lamothe et al., 2003; Huntley 2006; Kars et al., 2008). The first correction approach has been proposed and tested by **Huntley and Lamothe (2001)** and is applicable only for the liniar part of the dose response curve, corresponding to ages no older than 20-50 ka.

2.5 Protocols used for equivalent dose determination

Over the last years, a standard procedure (known in literature as "Single Aliquot Regenerative dose (SAR)") for equivalent dose determination has been developed. Following the general steps from the SAR procedure, measurement protocols have been developed and adapted to the dosimeter of choice. As such, when quartz is the preferred mineral, the standard single-aliquot regenerative dose

(SAR-OSL) protocol is used while for feldspars different protocols that use double IR stimulation at elevated temperature were developed in the general framework of the SAR protocol.

2.5.1 Single-aliquot regenerative dose (SAR-OSL) protocol

The general protocol used for quartz equivalent dose determination is the single-aliquot regenerative-dose optically stimulated luminescence (SAR-OSL) protocol developed by **Murray and Wintle (2000, 2003)** for fast component dominated quartz. The main steps of the SAR protocol are outlined in Figure 2.2.

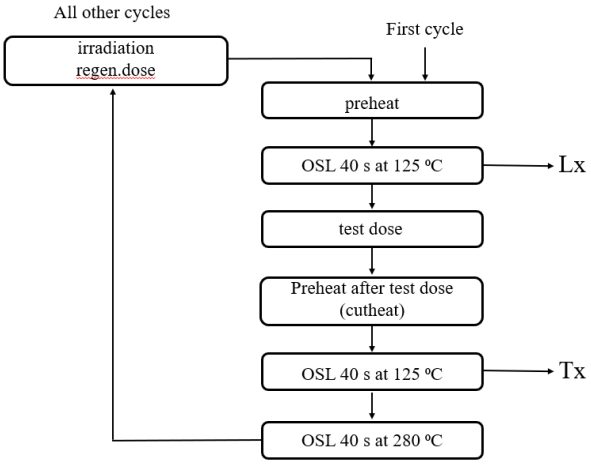

Figure 2.2 General steps of the single aliquot regenerative dose (SAR-OSL) protocol proposed by **Murray and Wintle (2000, 2003)**. Lx represents the natural or regenerated signal and Tx is the test dose signal.

The SAR-OSL protocol consists from a series of irradiations, thermal treatments and optical stimulations with blue diodes in order to construct a dose response curve. The performance of the SAR protocol is assessed for each aliquot used for measurement by using several intrinsic tests such as: the Recycling test used to evaluate the sensitivity changes during repeated cycles of the SAR protocol, the Recuperation test assess if exist thermal transfer of charge from the previous cycle to the next one and the IR depletion test which allows to evaluate the purity of the OSL signals emitted by quartz.

Additional investigations can be performed in order to confirm the validity of equivalent doses measured by using the SAR protocol. One of the tests that can be done is the preheat plateau test which assesses the effect of variation of the preheat temperature on the magnitude of the equivalent dose.

The most stringent test that can provide evidence for the applicability of the SAR protocol is the dose recovery test developed by **Murray and Wintle (2003)**. The

purpose of this test is to check if the SAR protocol can successfully measure a known artificial dose (induced in the laboratory).

Several studies reported age underestimation for sample older than 70 ka even though the aliquots passed all the intrinsic tests of the SAR protocol (e.g. **Buylaert et al., 2007; Lowick et al., 2010; Timar et al., 2010**). The best approach in evaluating the reliability of luminescence ages in general is to compare these ages with chronologies obtained independently (e.g., **Murray and Olley, 2002; Constantin et al., 2012; Veres et al., 2013; Anechitei-Deacu et al., 2014**).

Some studies proved that natural processes may influence the luminescence properties of quartz and make it unsuitable for OSL dating (**Adamiec, 2000; Duller et al., 2000; Duller 2004; Preusser et al., 2006; Moska and Murray 2006).**

Another limitation of the SAR protocol is related to the discrepancy observed between fine and coarse quartz equivalent doses and thus ages for loess samples collected from different regions of the world (e.g**. Timar-Gabor et al., 2011, 2012; 2015, 2017; Timar-Gabor and Wintle 2013; Constantin et al., 2014**).

Another intriguing fact is that the pattern of the dose response curves of fine and coarse quartz fraction was different and thus showing distinctive saturation characteristics, with fine quartz having higher saturation parameters (**Kreutzeur et al., 2012; Timar-Gabor et al., 2017; Avram et al., 2020**).

One of the main assumptions of the SAR-OSL protocol is that the laboratory dose response curve reproduces the signal growth in nature. However, studies reported a mismatch between the growth of the natural and laboratory dose response curve, with laboratory dose response curves reaching saturation for higher doses (**Chapot et al., 2012; Timar-Gabor and Wintle, 2013; Timar-Gabor et al., 2015b; Avram et al., 2020**).

2.5.2 Circumventing fading using pIRIR protocols

Post infrared-infrared (pIRIR) protocols were elaborated for polymineral fine grains as well as for K-feldspars. Because the IRSL signal emitted by feldspars are known to be hampered by anomalous fading (**Wintle 1973; Spooner, 1992; 1994**), the need for developing protocols that can circumvent this phenomenon was necessary.

The first step in the development of a protocol that precludes the signal loss was made by **Thomsen et al. (2008)**. They found that a second IR stimulation at a temperature of 225 °C given after the IR stimulation at 50 °C will lead to a much more stable IR signal (**Thomsen et al., 2008**). The IR stimulation at 50 °C is applied in order to reduce the neighbour trap-hole pairs which are susceptible to tunnelling while a consecutive IR stimulation at higher temperature will access more distant

trap-hole pairs which experience a signal with less fading (**Thomsen et al., 2008; Jain and Ankjaergaard, 2011; Poolton et al., 2002a, b**).

Therefore, two elevated temperature pIRIR protocols have been developed in order to reduce the signal susceptible to fading, namely $pIRIR_{225}$ (**Buylaert et al., 2009; Wacha and Frechen 2011**) and $pIRIR_{290}$ (**Thiel et al., 2011a; Buylaert et al., 2011, 2012**) (**Figure 2.3**).

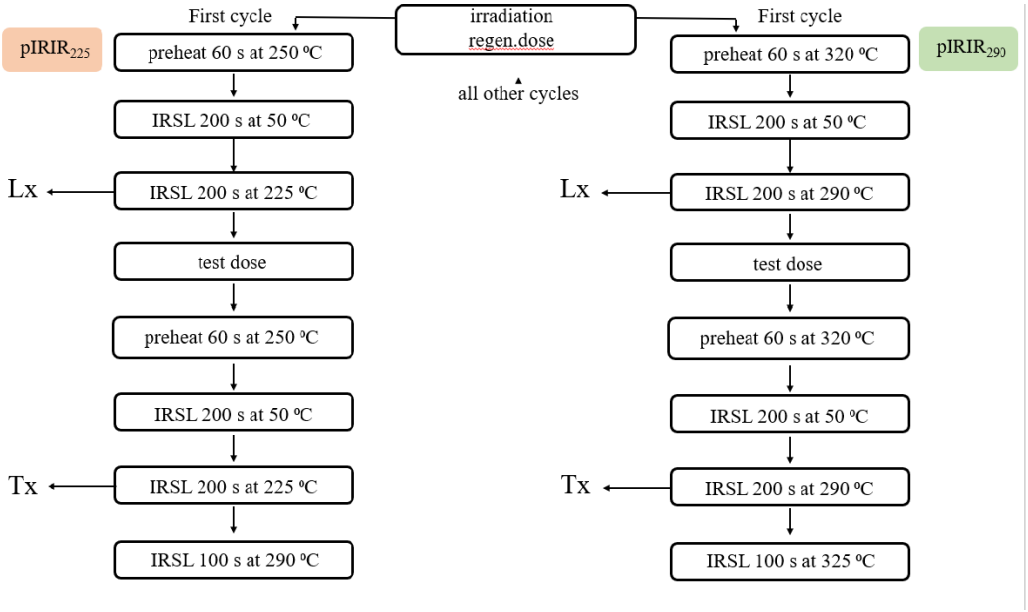

Figure 2.3 The schematic representation of the pIRIR protocols. In the left part of the figure is displayed the $pIRIR_{225}$ protocol while in the right part is presented the $pIRIR_{290}$ protocol. Lx represent the natural or regenerated IRSL signals while Tx is the test dose IRSL signal.

The capability of resetting the signal represents a pre-requisite for conducting accurate dating. Previous studies reported that pIRIR signals stimulated at high temperatures (e.g., $pIRIR_{225}$, $pIRIR_{290}$) are more difficult to bleach (e.g., **Thomsen, 2008; Buylaert et al., 2009; Thiel et al., 2011a**) and a residual dose of a few Gray is obtained even after a long exposure to sunlight or to the solar simulator. Therefore, residual signals that transpose in the residual doses play an important role when dealing with high-temperature pIRIR signals. The incorrect measurement of the remanent dose will lead to an equivalent dose overestimation.

In order to check the reliability of the doses measured by pIRIR protocols, both recycling and recuperation tests are incorporated in each measurement. These tests have the same applicability as those used in the SAR-OSL protocol for quartz. Beside the intrinsic tests of the SAR procedure, the most stringent test that can prove the robustness of a protocol is the dose recovery test (**Murray 1996; Wallinga et al., 2000**). This test has the same fundamental principle as that used for quartz. First, the

natural signal has to be erased by exposing the aliquots to sunlight or solar simulator. Further, a known beta dose equal with the magnitude of the equivalent dose is given and the pIRIR protocol is then applied in order to determine this given dose as an unknown dose. The ratio between the recovered and given dose should be ideally equal to unity, with an accepted 10% deviation.

3. Testing polymineral post-IR IRSL and quartz SAR-OSL protocols on Middle to Late Pleistocene loess at Batajnica, Serbia

3.1 Introduction

The Middle Danube basin comprises several high-resolution Middle to Late Pleistocene loess-paleosol sequences (LPS) that document clear similarity in the long-term palaeoclimate response between European and Asian loess deposits (**Buggle et al., 2009, 2013; Marković et al., 2015 and references therein**). The LPS of Batajnica (Vojvodina region, Serbia) is considered one of the most complete and thickest terrestrial palaeoclimate archives that exhibit five clearly distinguishable loess and palaeosol units, reaching to Marine Isotope Stage (MIS) 16 (**Figure 3.1**).

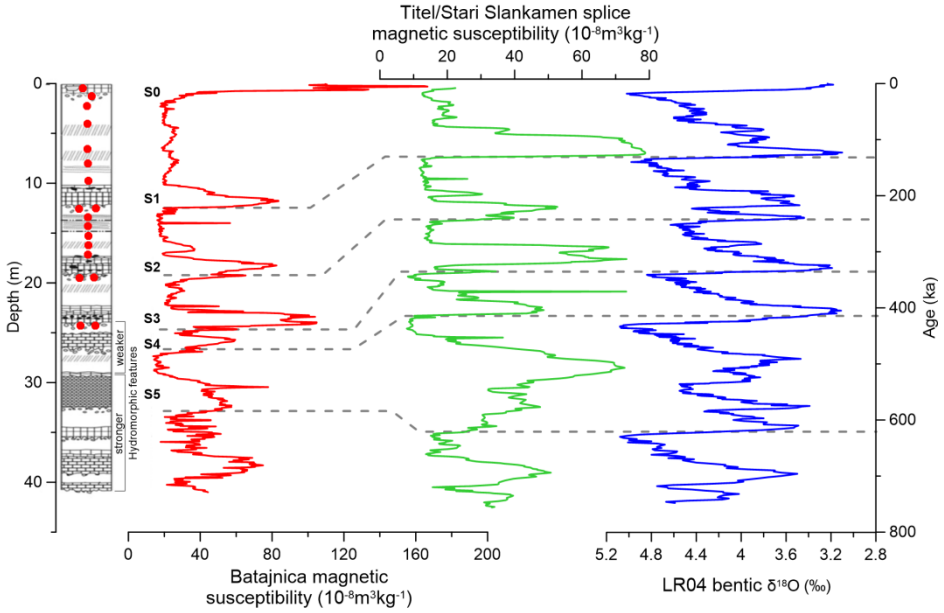

Figure 3.1 Stratigraphy and magnetic susceptibility of the Batajnica site (**Marković et al. 2009**) and its correlation to the astronomically tuned magnetic susceptibility record from the Titel/Stari Slankamen composite record (**Basarin et al. 2014**) and benthic oxygen isotope stack (**Lisiecki & Raymo 2005**).

Here we (i) provide a detailed multi-method luminescence chronology for the Batajnica profile with the focus on the last glacial loess unit; (ii) explore the upper dating limit of the single-aliquot regenerative dose (SAR) protocol applied on 4–11 and 63–90 μm quartz OSL, as well as $pIRIR_{290}$ and $pIRIR_{225}$ applied on 4–11 lm polymineral fine grains from samples collected from L1 (c.MIS 5–2) loess unit and at the lower boundaries of S1 (c.MIS 5),S2(c.MIS 7) and S3 (c.MIS 9) palaeosols;and (iii) compare the natural and laboratory generated quartz SAR-OSL and post-IR $IRSL_{225}$ and $IRSL_{290}$ dose response curves and thus assess what is the dose range over which each protocol provides reliable ages.

Luminescence investigations were carried out on 18 individual samples collected in stainless steel tubes from the same outcrops studied by **Marković et al. (2009**).

3.2 Methodology

The luminescence samples were prepared under low intensity red light conditions. Gamma spectrometry and water content measurements were carried out using material from the ends of each sample tube, whereas fine quartz (4–11 lm), coarse quartz (63–90 lm) and polymineral fine grains were extracted from the inner part.

Luminescence measurements were performed using TL/OSL Risø DA-20 readers.

Equivalent doses of fine (4–11 μm) and coarse (63–90 μm) quartz grains were determined using the single aliquot regenerative dose (SAR) procedure (**Murray & Wintle 2000, 2003**) while for polymineral fine grains two elevated temperature infrared stimulation methods based on the SAR procedure were used, namely $pIRIR_{290}$ (**Buylaert et al. 2011a, 2012; Thiel et al. 2011a**) and $pIRIR_{225}$ (**Roberts 2008; Buylaert et al. 2009; Wacha & Frechen 2011; Vasiliniuc et al. 2012**).

It is well known that major palaeosols within Eurasian LPSs exhibit a distinctive magnetic enhancement pattern, which is also reflected in grain size and colour proxies, that denotes the degree of pedogenesis, which in turn is hydroclimatically controlled. These patterns and their stratigraphical superposition allow for secure identification of major palaeosols and serve as independent chronostratigraphical markers that constitute the backbone of the loess chronostratigraphy in the wider Danube Basin and beyond (**Marković et al. 2015; Necula et al., 2015**). As such, the major loess–palaeosol transitions identified in Batajnica according to the magnetic susceptibility record were correlated to the corresponding ones in the Titel/Stari Slankamen composite profile (**Figure 3.1**). This approach (see **Basarin et al. 2014**) further enabled a correlation to the benthic oxygen isotope stack (**Lisiecki & Raymo 2005**). As the luminescence samples were collected from the same outcrop where the magnetic susceptibility samples were taken, previous field marks allowed for secure correlation of our samples and the magnetic susceptibility samples. Expected age estimates have been assigned to samples collected from the Holocene soil and palaeosol boundaries (BAT-1.0, 1.11, 1.12A, 1.16, 1.17 and 1.19A) based on the data reported by **Basarin et al. (2014)** and their correlation to benthic oxygen ages of **Lisieck i& Raymo (2005)** (**Figure 3.1**).

3.3 Results and discussion

3.3.1 Annual doses and calculation of expected equivalent doses

The annual doses were derived from the activity concentrations of the ^{238}U, ^{232}Th ^{40}K and ^{210}Pb measured using gamma spectrometry. We have investigated the secular equilibrium assumption in the ^{238}U chain by assessing the ratio between the activity concentration of ^{210}Pb measured directly using the 46 keV line and ^{226}Ra indirectly measured using the ^{214}Pb (352 and 295 keV) and ^{214}Bi (609.3 keV) energy peaks. Moreover, the activity concentration of ^{210} Pb was determined indirectly using alpha spectrometry by measuring ^{210}Po for 10 samples. The results showed that the ratios between gamma and alpha spectrometry data are consistent with unity. This indicates that ~50% radon loss occurs in the investigated samples. Thus, the annual doses used for age calculation were considered the measured ^{210}Pb.

By multiplying the expected age estimates by the corresponding environmental dose rate, expected equivalent doses and their associated uncertainties were determined.

3.3.2 Luminescence properties – quartz

For both fine and coarse quartz fractions the net signal displayed a rapid decay, similar with that of calibration quartz. The dose response curves (DRC) were well fitted using the sum of two saturating exponential functions. The aliquots used for equivalent dose calculation passed all the intrinsic tests of the SAR procedure.

Preheat plateau – the results showed that over the interval 180 to 280 °C of preheat temperature; equivalent doses do not display systematic variation.

Dose recovery – the dose recovery ratios showed that SAR protocol can successfully recover laboratory doses up to 320 Gy on fine quartz and 260 Gy on coarse quartz.

Equivalent doses - Equivalent doses measured on fine quartz aliquots range from 31±1 Gy for sample BAT-1.0 collected from the Holocene soil to 486±5 Gy for sample BAT-1.19A from below the S3 palaeosol. The natural signal emitted by this sample interpolates well below the laboratory saturation threshold. Coarse quartz equivalent doses range from 28±1 Gy for the sample from modern soil to 262±16 Gy for a sample collected below the S1 palaeosol. For older samples, the natural signal was in field saturation and close to laboratory saturation.

3.3.3 Luminescence properties – polymineral fine grains

The dose response curves constructed for both pIRIR protocols were well fitted using the sum of two saturating exponential functions and the growth curve pass very close to the origin, demonstrating that the recuperation is insignificant.

Effect of test dose size on equivalent dose - The effect of test dose size on the measured equivalent dose using the $pIRIR_{290}$ protocol was investigated on samples BAT-1.9, 1.12A and 1.16. For samples BAT-1.9 andBAT-1.12A no systematic trend in equivalent dose values with test dose magnitude can be seen. Although not so clear, this is also valid for sample BAT-1.16, which yielded $pIRIR_{290}$ equivalent doses of 1172±129 and 996±64 Gy by employing test dose sizes of 2 and 50% of the De, respectively. The expected equivalent dose for sample
BAT-1.16 is 617±84 Gy.

Determination of residual doses – Besides conducting laboratory bleaching experiments that consist in exposure the sample to sunlight or solar simulator, another way to derive the residual doses is by measuring a modern analogue. Firstly, the residual doses were measured after 1 moth exposure to the UV lamp. The measured residual values amount to a maximum of 0.5 and 4% of the measured $pIRIR_{225}$ and $pIRIR_{290}$ equivalent doses, respectively. As there was no modern analogue sample, we estimated the residual doses from the youngest sample ages BAT-1.0.These residual doses were subtracted from off pIRIR equivalent doses prior to age calculation.

Dose recovery- the $pIRIR_{225}$ protocol can successfully recover laboratory doses up to 316 Gy, while the $pIRIR_{290}$ protocol systematically overestimates the given laboratory doses. Following the suggestions of **Yi et al. (2016),** we carried out $pIRIR_{290}$ dose recovery tests using higher test doses. For sample BAT-1.9, the dose recovery ratio improved from1.36±0.06 to 1.07±0.03 using a 17 Gy test dose (7% of De) and a 50 Gy test dose (23% of De), respectively. However, for sampleBAT-1.11 poor dose recovery ratios of 1.31±0.04 and 1.41±0.10 were obtained by using test doses of 17 Gy (5% of De) and 150 Gy (41% of De), respectively. The size of the test dose does not influence the measured equivalent dose or the saturation characteristics of the $pIRIR_{290}$ dose response curves.

Polymineral fine grains equivalent doses – The $pIRIR_{290}$ equivalent doses vary from 36±9 Gy (BAT-1.0) to 490±21 Gy (BAT-1.12A). The smallest $pIRIR_{225}$ equivalent dose is 37±6 Gy (BAT-1.0), whereas the maximum is 377±19 Gy (BAT-1.12A). The natural $pIRIR_{225}$ and $pIRIR_{290}$ signals yielded by older samples scatter around or above the saturation threshold of the dose response curve.

Fading rate measurements for high doses – Fading rates were measured for samples BAT-1.11 and BAT-1.19A. Our results show a significant scatter in the pIRIR

sensitivity-corrected luminescence signals registered during prompt read-outs. It is interesting to note that the signal intensity recorded after the first instantaneous read-out always lies above the values recorded during the subsequent prompt read-outs. We consider that no systematic variation with delay time is identified for the pIRIR sensitivity-corrected luminescence signals. Moreover, a fading test was performed on both fine and coarse quartz which is well known that quartz does not suffer from anomalous fading (**Aitken 1998**). We report average g-values of 2.49±0.44 and 2.92±0.61%/decade for 4–11 and 63–90 μm quartz, respectively. Such g-values cannot reflect real fading as this would imply a significant signal loss during burial. This is in contradiction with our observation that the natural signals emitted by 63–90 μm quartz are close to full saturation, as discussed below.

High laboratory doses given on top of naturally accrued doses - If large laboratory doses are added on top of natural signals found in field saturation, an increase of the signals may suggest a degree of fading that may have been undetected during standard fading rates measurements. On the other hand, if a large dose is given on top of the naturally accrued doses, one normally expects the magnitude of the measured signal to be the same as the saturation value measured in the SAR protocol. We have perform such an experiment on sample BAT-1.19A, with an expected age of more than 300 ka and natural signals close or in laboratory saturation. The ratios between the sensitivity corrected luminescence signal measured after a dose of 5000 Gy was added on top of the natural $(L_n/T_n)^*$ and the sensitivity corrected luminescence signal of the natural dose (L_n/T_n) is 1.90±0.02 in the case of fine grains and 0.96±0.08 in the case of coarse grains. For polymineral fine grains the ratio of $(L_n/T_n)^*$ to (L_n/T_n) is 1.35±0.03 in the case of $pIRIR_{225}$ and 1.20±0.04 in the case of $pIRIR_{290}$. The ratio between $(L_n/T_n)^*$ and (Lx/Tx) in the case of $pIRIR_{225}$ is 1.10±0.03 while for $pIRIR_{290}$ is 1.15±0.05. In the case of fine and coarse quartz corresponding ratios of 0.95±0.02 and 1.03±0.11, respectively, were obtained. This indicates that in the case of all signals excepting coarse quartz OSL the maximum light levels attained during prolonged natural irradiation can be increased by additional laboratory irradiation.

3.3.4 Luminescence ages

The ages calculated using the measured activity concentrations of ^{210}Pb are generally 10 to 20% older than those calculated assuming secular equilibrium in the ^{238}U chain, but the two sets of ages are consistent within error limits. Assuming a constant radon loss over the whole sample burial time, the set of ages calculated using the measured activity concentrations of ^{210}Pb is discussed.

For Batajnica, the luminescence ages are in agreement with the previous chronological framework based on magnetic susceptibility correlation to other records (**Buggle et al. 2009; Marković et al. 2009**), placing the L1 loess unit into the Last Glacial. Except for sample BAT-1.9, all fine quartz ages are systematically lower than coarse quartz ages and the difference between them increases with depth (**Figure 3.2**), with the fine quartz underestimating the expected depositional ages based on magnetic stratigraphy. The coarse quartz, polymineral $pIRIR_{225}$ and $pIRIR_{290}$ ages largely agree (**Figure 3.2**) and within errors are consistent with the expected ages. Immediately below the S1 palaeosol, the coarse quartz, $pIRIR_{225}$ and $pIRIR_{290}$ yielded ages up to 116±12 ka (262±16 Gy), 130±14 ka (377±19 Gy) and 169±17 ka (490±21 Gy), respectively.

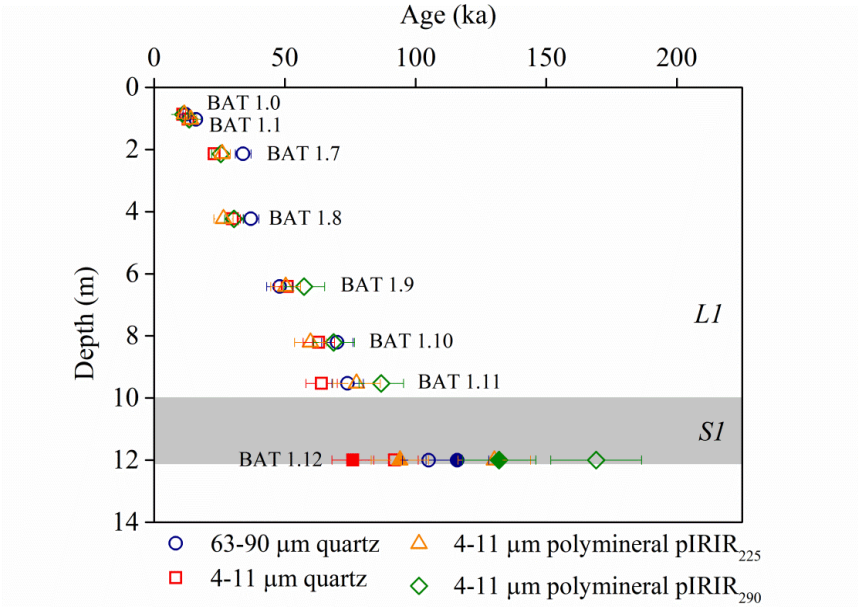

Figure 3.2 Quartz OSL and polymineral $pIRIR_{225}$ and $pIRIR_{290}$ ages for the uppermost loess-palaeosol alternation in Batajnica site. Note the doublet samples collected at 12 m depth: open symbols indicate sample BAT-1.12A while filled symbols represent sample BAT-1.12B.

For samples taken from deeper units (BAT-1.13A to 1.19A, B), except for fine quartz, the natural signal is in the region of laboratory saturation.

3.3.5 Accuracy of the reported luminescence ages

In order to identify the factors that control the upper limit of luminescence dating we investigate the saturation characteristics of the natural and laboratory signals emitted by both quartz and polymineral grains

Laboratory dose response curves.

Laboratory dose response curves (DRC) up to 5000 Gy were constructed on sample BAT-1.19A collected from below the S3 palaeosol (>300 ka according to **Marković et al., 2009**) using 4–11 and 63–90 μm quartz as well as polymineral fine grains employing the $pIRIR_{225}$ and $pIRIR_{290}$ protocols. All dose response curves were best fitted with the sum of two saturating exponential functions. Following the suggestion of **Wintle & Murray (2006)** we consider the saturation threshold at 85% of the laboratory dose response curve. We assess the closeness to saturation of natural signals by calculating the ratios between the average sensitivity-corrected natural signals (L_{nat}/T_{nat}) and the corrected luminescence signals measured for the 5000 Gy regenerative dose ($Lx/Tx_{5000\ Gy}$).

The laboratory DRC on coarse quartz saturates earlier than fine quartz and polymineral samples and has saturation characteristic doses of D_{01} = 21±28 Gy and D_{02} = 153±46 Gy. The coarse quartz natural signal reaches laboratory saturation (**Figure 3.3**). Fine quartz on the other hand, yields a laboratory luminescence signal that continues to grow to doses beyond 5000 Gy and the natural signal is interpolated well below the saturation region of the dose response curve. The characteristic doses for fine quartz dose response curves are D01 = 178±17 Gy and D02 = 1635±164 Gy.

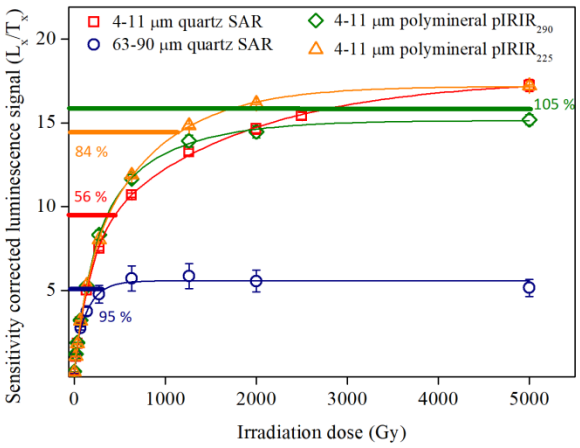

Figure 3.3 Laboratory dose response curves constructed for 4-11 μm and 63-90 μm quartz, 4-11 μm polymineral grains measured with $pIRIR_{225}$ and $pIRIR_{290}$ protocols on sample BAT-1.19A (> 300 ka). The average L_{nat}/T_{nat} obtained on all aliquots measured, including De measurements, is interpolated on the growth curve. The percentage indicated for each interpolation represents the ratio between the L_{nat}/T_{nat} and the L_x/T_x measured for the 5000 Gy regenerative dose.

It is important to note that $pIRIR_{225}$ and $pIRIR_{290}$ laboratory dose response curves have lower characteristic doses than the fine quartz. We report D01 = 142±13 Gy and D02 = 795±36 Gy for $pIRIR_{225}$ while for $pIRIR_{290}$ D01 = 193±32 Gy and D02 = 764±145 Gy. The natural $pIRIR_{225}$ signal of sample BAT-1.19A is 84±0.7% of laboratory saturation while the$natural pIRIR_{290}$ signal is 105±3% and lies slightly above the light level corresponding to the 5000 Gy dose (**Figure 3.3**).

The influence of the magnitude of the test dose on the $pIRIR_{290}$ laboratory growth curves was also documented. Based on our finds for Batajnica, we conclude that the dependence of the saturation parameters on the size of the test dose reported for Chinese loess (**Yi et al. 2016**) or fluvial sediments from South Africa (**Colarossi et al. 2018**), might not represent a general feature of $pIRIR_{290}$ laboratory signals.

In order to quantify the closeness of the natural sensitivity-corrected luminescence signals to laboratory saturation for all samples collected from the deeper units (BAT-1.12A-BAT-1.19B), we calculated the ratio between the natural sensitivity-corrected luminescence signal and the average maximum corrected luminescence signals induced by a dose of 5000 Gy.

Natural dose response curves

In order to assess the reliability of the luminescence ages, natural and laboratory dose response curves were compared. Fine grained quartz natural and laboratory growth curves overlap until ~150 Gy (**Figure 3.4a**). This suggests that fine quartz natural signals resulting from doses up to ~150 Gy (c. 50 ka) could result in reliable ages. For higher natural doses the SAR protocol underestimates the expected fine quartz equivalent doses. Coarse-grained quartz natural and laboratory growth curves overlap until ~250 Gy, corresponding to an upper age limit of c. 100 ka for the Batajnica samples (**Figure 3.4b**). This implies that for natural doses up to 250 Gy (c. 100 ka), the SAR protocol provides reliable coarse quartz OSL ages.

The uncorrected $pIRIR_{225}$ natural and laboratory growth curves appear to generally overlap over the dose range investigated (up to ~1200 Gy; **Figure 3.4c**). However, the overlap beyond ~500 Gy should be interpreted with caution because of the large errors of the data points and their spread along with our observation that the natural signals are in field saturation.

The natural $pIRIR_{290}$ signals are consistent with the laboratory signals for doses up to ~400 Gy (**Figure 3.4d**). For higher doses, the natural $pIRIR_{290}$ signals overestimate the laboratory signals for the Batajnica samples. The $pIRIR_{225}$ and $pIRIR_{290}$ natural signals of samples collected from L2 were found to be in both field and laboratory saturation.

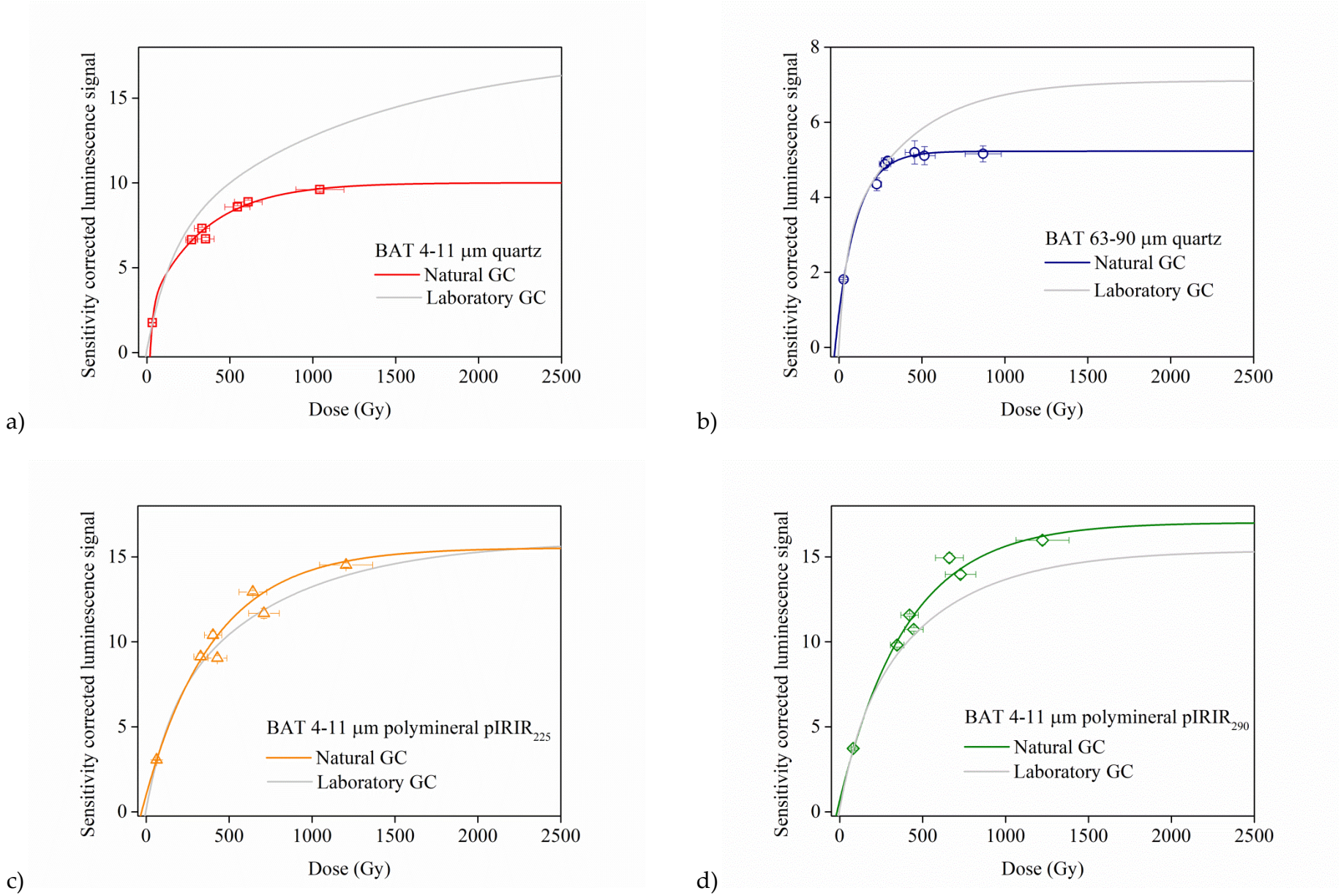

Figure 3.4. Average of natural sensitivity corrected luminescence signals emitted by **(a)** 4-11 µm and **(b)** 63-90 µm quartz, 4-11 µm

polymineral grains measured with **(c)** $pIRIR_{225}$ and **(d)** $pIRIR_{290}$ protocols, plotted as function of expected equivalent doses for the samples collected from the loess/paleosols boundaries (BAT-1.0, BAT-1.11, BAT-1.12A, BAT-1.12B, BAT-1.16, BAT-1.17, BAT-1.19A). The expected equivalent doses are derived from the magnetic susceptibility data correlated to the benthic oxygen stack (**Lisiecki and Raymo, 2005**). The average laboratory dose response is presented for comparison. Data are fitted by a sum of two saturating exponential functions. Please note the small vertical uncertainties on the corrected natural light levels.

3.4 Conclusion

Luminescence dating of 63–90 μm quartz and 4–11 μm polymineral grains using the $pIRIR_{225}$ protocol provided age estimates for the LGC at Batajnica. The 63–90 μm quartz ages are reliable up to 100 ka before exhibiting field and laboratory saturation. The 4–11 μm quartz yields reliable ages only for MIS 2 loess samples and increasingly underestimates the true depositional time for older samples. The $pIRIR_{225}$ and $pIRIR_{290}$ protocols applied on 4–11 μm polymineral grains provide reliable ages over the last glacial cycle (LGC), beyond which they are in field and laboratory saturation.

The upper limit of the luminescence dating methods at Batajnica is imposed by saturation of the natural signals starting with samples collected from L2 loess (BAT-1.13A-1.19A, B).

The comparison between the natural and laboratory dose response curves predicts the dose range over which reliable luminescence ages are obtained for each signal investigated. For 4–11 and 63–90 μm quartz, the natural and laboratory dose response curves overlap until ~150 and ~250 Gy, respectively, while for $pIRIR_{225}$ there is an apparent overlap of the natural growth curve up to at least 500 Gy. The $pIRIR_{290}$ natural and laboratory growth curves are consistent with the laboratory dose response curve up to doses of 400 Gy beyond which the natural signals overestimate the laboratory signals.

4. Optically stimulated luminescence dating of loess in South-Eastern China using quartz and polymineral fine grains

4.1 Introduction

The widespread loess deposits to the south of the Chinese Loess Plateau, distributed in the subtropical region of East Asia (**Jiang et al., 2020**) constitute well-preserved paleoclimate records (**Hao et al., 2010**). These archives are widely spread in the middle and lower reaches of the Yangtze River as well as in the Huai River region recording changes starting from the Mid-Pleistocene Transition (**Qiao et al., 2003; X. Li et al., 2018; Wang et al., 2018**). The loess-paleosol sequences occurring in this region are collectively termed as "*Xiashu* loess" (**Han et al., 2019 and references therein**).

This study aims to provide the first numerical chronology for a loess-paleosol profile from Huai River valley, southeastern China. Therefore, luminescence dating method using three protocols was applied on quartz and polymineral fine grains extracted from eight samples. Moreover, the three sets of ages are compared with the magnetic susceptibility records as well as with the lithological information.

4.2 Study area

Eight luminescence samples were collected from a typical loess-paleosol sequence located within the hilly region (mainly eastern end of Zhangba Hills) in the drainage area of the Huai River; the investigated loess-paleosol profile is termed here as XuYi (XY) section (118° 39.361′ E, 32° 50.990′ N) and is located in the XuYi county, the Jiangsu Province, southern China. The total exposure of the sequence reaches a thickness of ~6 m.

4.3 Experimental details

4.3.1 Lithology and magnetic susceptibility data

At the XuYi (XY) section, two glacial units L1 and L2 as well as the interglacial pedocomplex S1 are easily identified based on magnetic susceptibility data (**Figure 4.1)**. The whole section has experienced strong paedogenesis, and the lithological divisions are made by relative changes in the paedogenic intensity. The lithological information is presented in **Figure 4.1**.

The variations recorded in magnetic susceptibility for loess-paleosol deposits in the Chinese Loess Plateau reflect palaeo-environmental changes during glacial and interglacial periods. Thus, an enhancement of the ferromagnetic minerals in loess is correlated with the paedogenetic process which took place during

interglacial periods. By contrast, the concentration of ferromagnetic minerals decreases considerably in the glacial periods. Therefore, the magnetic susceptibility variations can be correlated with deep-sea oxygen isotope records (e.g., **Liu, 1985; An et al., 1991; Lu et al., 1999; Hao et al., 2012**). The magnetic susceptibility (MS) analysis was carried out on 246 samples collected from the XY loess-paleosol sequence at a resolution of 2.5 cm. The variations recorded in the low-field MS display crucial information about the XY pedostratigraphy. The complete MS record is presented in **Figure 4.1**.

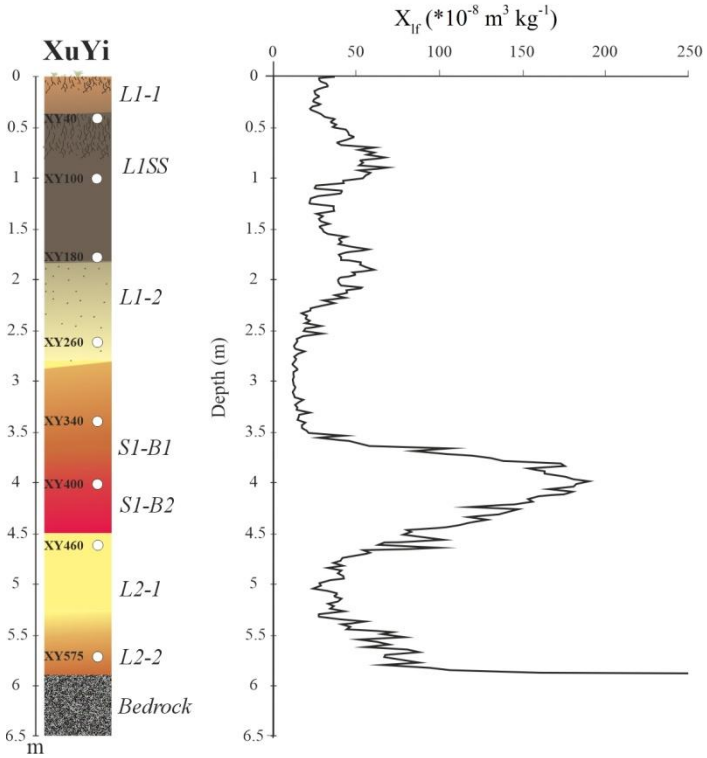

Figure 4.1. Stratigraphy and magnetic susceptibility (MS) records of XuYi (XY) loess-paleosol sequence. The stratigraphical positions of luminescence samples are displayed with circle symbols in the stratigraphical column.

4.3.2 OSL dating

Sample preparation and measurement technique

Luminescence samples were prepared under subdued red-light laboratory conditions. The material was used for 4-11 μm quartz and polymineral fine grains extraction.

Luminescence investigations were carried out using two TL/OSL Risø DA-20 readers equipped with either classic or automated, detection and stimulation head (DASH) (**Lapp et al., 2015**).

Equivalent dose determination

Quartz equivalent doses (De) were determined using a standard single aliquot regenerative dose (SAR) protocol (**Murray and Wintle, 2000, 2003)** while equivalent dose determination on polymineral fine grains was carried out using two elevated temperature post-infrared infrared stimulation methods based on SAR procedure, namely the $pIRIR_{225}$ (**Roberts 2008; Buylaert et al., 2009; Wacha and Frechen 2011; Vasiliniuc et al., 2012**) and $pIRIR_{290}$ (**Buylaert et al., 2011a, 2012; Thiel et al., 2011a**) protocols.

4.4 Results and discussion

4.4.1 Luminescence characteristics

4.4.1.1 Quartz OSL

The equivalent doses were obtained by interpolating the sensitivity corrected natural OSL signal onto the dose response curve. The natural OSL signal decayed significantly within the first second of stimulation, exhibiting a similar pattern to that of the decay measured for calibration quartz which is accepted as being dominated by the fast component (**Hansen et al., 2015**). The aliquots used for age calculation passed all the intrinsic tests of the SAR protocol.

Preheat plateau test – the observed equivalent doses display a slight variation for thermal treatments between 180 °C and 280 °C suggesting that the equivalent dose values show a small dependence of preheat temperatures, however as there is no definite trend and given the dose recovery test results presented below, the middle value of 220 °C was chosen as the preheat temperature.

Dose recovery test - dose recovery ratios were satisfactory for all samples documented here, indicating that laboratory doses up to 474 Gy given prior to any heat treatment are accurately measured using the SAR protocol.

4.4.1.2 Polymineral fine grains – $pIRIR_{225}$ and $pIRIR_{290}$

The equivalent doses on polymineral fine grains were obtained by applying $pIRIR_{225}$ and $pIRIR_{290}$ protocols.

Residual doses

Residual doses were measured on aliquots that were exposed for 30 days under natural conditions on a window. The magnitude of the residual doses measured using $pIRIR_{225}$ protocol range from 2.0±0.1 to 9±1 Gy while the $pIRIR_{290}$ residual doses are larger and vary between 4±1 and 19±3 Gy. The results show a dependency between the residual dose and the equivalent dose values (**Figure 4.2**).

This can be explained if one assumes that the time used in the bleaching experiment was not long enough for the signal to be fully reset, in other words the exposure was not long enough for the signal to reach a constant value. In this case, the intercept of the linear fit between the measured residual and the equivalent dose corresponds to the component that could not be zeroed by light exposure. For our samples, the intercept dose is the most appropriate value to be subtracted. An intercept dose of ~ -0.02±1.3 Gy was obtained for pIRIR$_{225}$ protocol (see inset **Figure 4.2**) while for the pIRIR$_{290}$ protocol a value of 2.8±1.7 Gy was determined (see inset **Figure 4.2**). Considering the small aforementioned values determined, that are consistent to zero within uncertainties, the pIRIR luminescence ages were further determined without any residual correction.

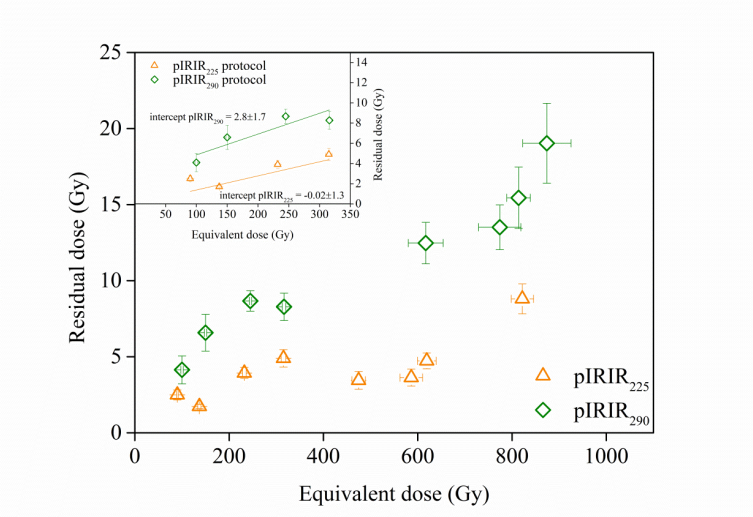

Figure 4.2 Residual doses measured after an exposure of 30 days to window light as function of measured equivalent doses. The inset shows the values obtained for the samples with equivalent doses of less than 316 Gy fitted by a linear function.

Dose recovery test

The accuracy of the measurement pIRIR protocols have been assessed for doses that vary between 80 and 800 Gy. As such, for pIRIR$_{225}$ protocol, sets of five aliquots were irradiated with doses of 88, 135, 300, 400, 600 and 800 Gy while beta doses of 96, 143, 200, 300, 400, 600 and 745 Gy were given for aliquots that were measured using pIRIR$_{290}$ protocol. The dose recovery ratios for pIRIR$_{225}$ protocol measured for given doses up to 300 Gy range from 1.02±0.05 for a given dose of 88 Gy to 1.09±0.04 for a dose of 300 Gy. For higher given doses (> 400 Gy), dose recovery ratios start to overestimate by ~17-40% (**Figure 4.3a**). In the case of pIRIR$_{290}$ protocol, dose recovery ratios of 1.12±0.04 were obtained for given doses up to 200 Gy, a ratio of 1.18±0.07 was obtained for a dose of 300 Gy while for doses higher than 400 Gy, dose recovery ratios overestimate unity by ~30 to 60% (**Figure 4.3b**).

Furthermore, the dependency of the dose recovery ratios on the magnitude of the test dose was checked for both pIRIR protocols. In the case of pIRIR$_{225}$ protocol, sets of three aliquots were irradiated with beta doses of 300, 400, 600 and 800 Gy. These dose recovery measurements were performed using a test dose of 50% of the given dose. On the other hand, the influence of a test dose of 50% of the given dose was investigated for pIRIR$_{290}$ protocol for given laboratory doses of 300, 400, 550, 800 and 855 Gy. Moreover, two sets of three aliquots were irradiated with 855 Gy in order to measure the recovered doses with a test dose of 2% and 30% of the given dose. Further, five aliquots were irradiated with a beta dose of 143 Gy and the dose recovery ratio was obtained by measuring the recovered doses using a test dose of 12% of the given dose. Our results show that dose recovery ratios measured using pIRIR$_{225}$ protocol overestimate unity by ~11-33% for a range of doses between 400 Gy and 800 Gy (**Figure 4.3a**). In the case of pIRIR$_{290}$ protocol, our results demonstrate that an overestimation between 12 and 46% is identified for the entire dose range investigated here (**Figure 4.3b**).

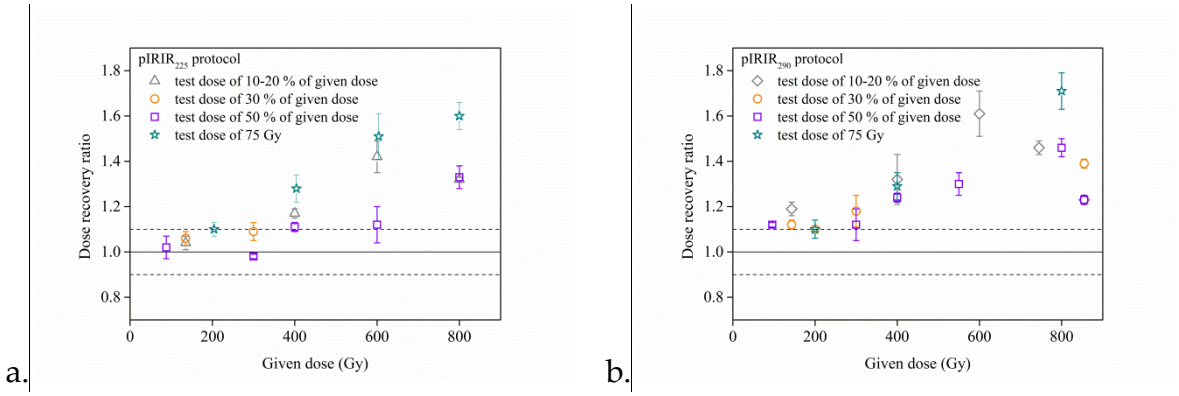

Figure 4.3. The results of dose recovery test using: (a) pIRIR$_{225}$ protocol and (b) pIRIR$_{290}$ protocols on 4-11 μm polymineral aliquots. Different symbols denote the use of different test dose values. The dose recovery test results when the given doses were added on top of the natural dose are represented with star symbols. For that experiment the test dose used was 75 Gy.

In order to avoid the potential complications due to inaccurate residual dose estimation, a dose recovery test can be performed by adding different beta doses on top of the natural signal of a young sample. The dose recovery ratios are further calculated by dividing the measured dose with the sum of the natural (i.e., previously determined equivalent dose) and the additional given dose (**Buylaert et al., 2011b, Yi et al., 2018**).

In this study, the uppermost sample XY 40 (measured De of ~97 Gy using pIRIR$_{290}$ protocol and ~101 Gy using pIRIR$_{225}$ protocol) was chosen and beta doses of

103, 303, 503 and 703 Gy as well as 99, 299, 499 and 699 Gy were added on top of the natural signals when $pIRIR_{290}$ and $pIRIR_{225}$ protocols were used. As such, the dose recovery test was carried out for total doses ranging from 200 to 800 Gy. The dose recovery ratios increase from 1.10±0.04 for a total dose (natural+given dose) of 200 Gy to 1.71±0.08 for a dose of 800 Gy for $pIRIR_{225}$ protocol (**Figure 4.3a**). In the case of $pIRIR2_{290}$ protocol the dose recovery ratios increase from 1.12±0.03 for a total dose (natural+given dose) of 200 Gy to 1.60±0.06 for a total dose of 800 Gy (**Figure 4.3b**). This confirms our previous observations in the dose recovery experiment performed using bleached aliquots. These results suggest that doses up to 200-300 Gy can be accurately measured with both pIRIR protocols while doses larger than 400 Gy are overestimated.

Fading

Previous studies reported that $pIRIR_{290}$ signal is stable and ages do not need any further correction for fading (e.g. **Thiel et al., 2011a; Buylaert et al., 2011a; Stevens et al., 2011**). Fading test was conducted only for $pIRIR_{225}$ protocol using doses of 100 Gy and 300 Gy, respectively. Storage time between 2 and 50 days were used. An average g-value smaller than 0.7 %/decade was obtained for all samples investigated here. Fading rates measured for each aliquot are spreading within a wide range of values for sample XY40 (from -0.97 to 4.22 %/decade), while for the other sample (XY100 and XY340) the variation measured for each aliquot is smaller. Based on our results as well as on the findings reported so far in literature (e.g. Vasiliniuc et al., 2012; Avram et al., 2020), in the following sections the uncorrected pIRIR ages are further discussed.

4.4.1.3 Saturation characteristics of quartz and feldspars signal

In order to assess the saturation characteristics of the laboratory signals of each protocol, dose response curves up to saturation need to be constructed (**Timar-Gabor and Wintle, 2013; Timar-Gabor et al., 2017; Anechitei-Deacu et al., 2018**). Therefore, DRC curves up to 5000 Gy were constructed for 4-11 μm quartz and polymineral on sample XY575, using SAR-OSL, $pIRIR_{225}$ and $pIRIR_{290}$ protocols. We assume a saturation threshold of 85% of the saturation level of the signal (**Wintle and Murray, 2006**). In order to evaluate the closeness to saturation of sample XY575 with equivalent doses >800 Gy, the ratios between the average sensitivity-corrected luminescence signals (L_{nat}/T_{nat}) and the corrected luminescence signal measured for a regenerative dose of 5000 Gy $(L_x/T_x)_{5000\ Gy}$ were calculated as for this dose it can be clearly seen that the dose response curves reach saturation. The natural OSL signal of fine quartz is interpolated at ~58±1% of the signal obtained for a dose of 5000 Gy.

The natural $pIRIR_{225}$ signal of sample XY575 is interpolated at 68±1% of the saturation level while the natural $pIRIR_{290}$ signal is interpolated at 81±3% of the saturation level.

The laboratory DRC constructed on fine quartz has characteristics saturation doses of D_{01} = 117±33 Gy and D_{02} = 1201±170 Gy. In the case of $pIRIR_{225}$ the saturation characteristics of the dose response curve are D_{01} = 175±15 Gy and D_{02} = 1094±53 Gy while for $pIRIR_{229}$ values of D_{01} = 150±39 Gy and D_{02} = 795±98 Gy were obtained.

4.4.1.4 High laboratory doses added on top of the natural signal

Previous studies demonstrated that the application of the SAR-OSL procedure is problematic in the high dose range (**Timar-Gabor et al., 2017; Anechitei et al., 2018, Veres et al., 2018; Avram et al., 2020**). When large laboratory doses are added on top of the naturally accrued doses, the magnitude of the measured signal is expected to be at the same level as the saturation signal measured in the SAR procedure.

Such an experiment has been conducted for sample XY180 on fine and polymineral fine grains using each protocol investigated in this study. As such, a beta dose of 5000 Gy was given on top of the natural dose (~200 Gy).

In the case of fine quartz, the ratio between the natural+given dose sensitivity corrected OSL signal $(L_n/T_n)^*$ and sensitivity corrected OSL signal of 5000 Gy (L_x/T_x) is 0.94±0.04 (**Figure 4.4**). The ratio between the (Ln/Tn)* and (Lx/Tx) in the case of $pIRIR_{225}$ is 1.11±0.04 while in the case of $pIRIR_{290}$ the ratio is 1.18±0.09 (**Figure 4.4)**.

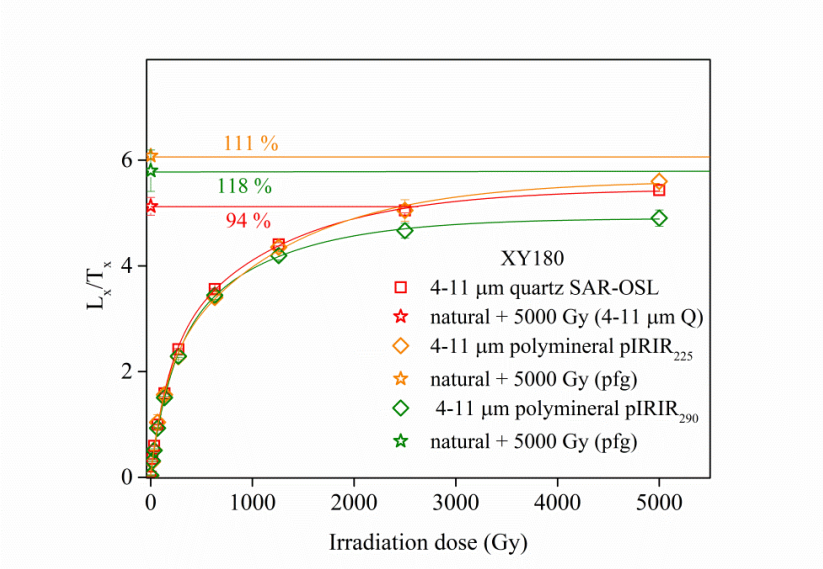

Figure 4.4 Laboratory dose response curves constructed for 4-11 µm quartz and polymineral grains measured using $pIRIR_{225}$ and $pIRIR_{290}$ protocols on sample XY180. All growth curves were best fitted by a sum of two saturating exponential functions.The average natural+5000 Gy sensitivity corrected signals $(L_n/T_n)^*$ are

interpolated onto the DRCs. The percentage indicate the ratio between the $(L_n/T_n)^*$ and the L_x/T_x measured for a regenerative dose of 5000 Gy.

These results are pointing out that for large doses fine quartz natural signal underestimates the true depositional dose. In the case of pIRIR protocols, the results reinforce the overestimation observed in the dose recovery tests presented above, indicating that the signals measured during the first measurement cycle slightly overestimate the signal obtained for a dose with the same magnitude given later in the SAR protocol. The $pIRIR_{290}$ overestimation is larger than in the case of $pIRIR_{225}$, as previously reported.

4.4.2 Luminescence ages

All three sets of ages are generally in agreement with each other up to ~70 ka and no reversals occur (**Figure 4.5)**. The pIRIR ages are consistent with each other up to 70 ka. In the case of $pIRIR_{225}$ protocol, ages from 20±2 ka to 65±6 ka were obtained while $pIRIR_{290}$ ages range from 23±2 ka to 67±5 ka (**Figure 4.5**)

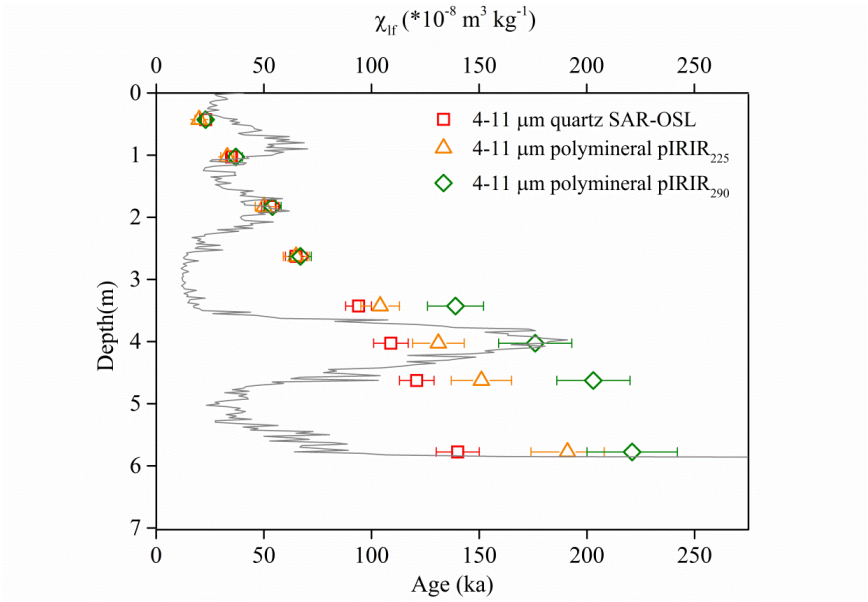

Figure 4.5 Magnetic susceptibility record and the three sets of ages obtained on quartz and polymineral fine grains using SAR-OSL and pIRIR protocols, respectively presented as function of depth.

Based on the results obtained in this study, we are confident that the three sets of ages on quartz and polymineral fine grains are reliable up to ~70 ka. Beyond this interval, the quartz SAR-OSL ages should be regarded as underestimated whereas polymineral pIRIR ages slightly overestimate the true depositional age.

4.5 Conclusion

High-resolution luminescence dating on 4-11 μm quartz and polymineral grains using SAR-OSL, $pIRIR_{225}$ and $pIRIR_{290}$ protocols have been applied on *Xiashu* loess deposits accumulated within the drainage area of the Huai River in southern China. Luminescence characteristics of quartz as well as of polymineral grains displayed a good behaviour in the SAR procedure for doses up to ~300-400 Gy. Luminescence ages obtained on fine quartz using SAR-OSL protocol and on polymineral fine grains using $pIRIR_{225}$ and $pIRIR_{290}$ protocols are consistent with each other up to ~70 ka, and thus confirming that the first layer of aeolian dust within the investigated region was accumulated during the last Glaciation. For samples with higher equivalent doses, the SAR-OSL protocol applied on quartz underestimate the true depositional ages whereas the ages obtained using both pIRIR protocols are interpreted as overestimate, an interpretation supported by the results obtained in dose recovery tests.

5. Investigations on the luminescence properties of quartz and feldspars extracted from loess in the Canterbury Plains, New Zealand South Island

5.1 Introduction

Archives in New Zealand play an important role for palaeo-climate reconstruction in the Southern Hemisphere (**Alloway et al., 2007**). Despite the well-established chronology of the North Island, there are few dating studies on the South Island of New Zealand.

The applicability of the OSL dating has been assessed on relatively few studies reported on sediments from the South Island of New Zealand. However, there is evidence that quartz from South Island suffers from major problems that limit its application, namely the weak sensitivity of the signal, with the signal apparently arising from many dim grains and the unsatisfactory behaviour in the SAR protocol (**Preusseur et al., 2006).**

The aim of this study is to further explore the luminescence properties of quartz extracted from a loess deposit from Canterbury Plains, in the South Island, and to assess the applicability of two pIRIR stimulated luminescence protocols on polymineral fine grains extracted from the same samples.

5.2 Study site

The study site (44.018870°S, 171.882054°E) is located in the southern Canterbury Plains, on the eastern side of central South Island.

For luminescence investigations, five samples were collected from the top section of the flank. The uppermost sample was discarded from the analysis due to its proximity to the modern disturbed surface.

5.3 Methodology

5.3.1 Sample preparation

Sample preparation was carried out under red-light laboratory conditions. Polymineral fine grains as well as coarse (63-90 μm, 90-125 μm, 125-180 μm and 180-250 μm) quartz grains were extracted.

5.3.2 Analytical Facilities

All luminescence measurements were carried out using two Risø TL/OSL readers (model DA-20), equipped with a classic or automated detection and stimulation head (DASH) (**Lapp *et al.*, 2015**).

Raman spectra have been recorded using a Renishaw InVia Reflex Confocal Raman system with a Leica microscope using the 100× (NA 0.9) long working-distance objective.

5.3.3 Equivalent dose determination

The single-aliquot regenerative-dose optically stimulated luminescence (SAR-OSL) protocol (**Murray and Wintle 2000, 2003**) was applied on coarse quartz grains. Equivalent doses measured on polymineral fine grains were carried out by applying two elevated-temperature infrared-stimulation methods based on the SAR procedure and the $pIRIR_{225}$ (**Buylaert *et al.*, 2009; Wacha and Frechen, 2011; Vasiliniuc *et al.*, 2012**) and $pIRIR_{290}$ (**Buylaert *et al.*, 2011a, 2012; Thiel *et al.*, 2011a**) protocols.

5.4 Results and discussion

5.4.1 Luminescence properties – Quartz

To check if the quartz extracted from the investigated samples is suitable for OSL dating, the SAR-OSL protocol was applied. The decay of the natural signal and the signal induced by a dose of 100 Gy was compared to that of the calibration quartz. The results showed that the fast component does exist in the OSL signal but its intensity is very weak. All investigated grain sizes displayed low sensitivity, with no more than 1500 cts recorded in the first 1.2 s of stimulation in the case of the natural signal.

The SAR protocol has been applied on various grain sizes but significant sensitivity changes were observed to occur. The response to the administered test dose was found to vary significantly from one cycle to another, the response increasing significantly during measurement cycles. The SAR protocol is not able to correct for sensitivity changes and a well-defined dose response curve could not be constructed; an example of this can be observed in **Figure 5.1.** Therefore, equivalent doses could not be confidentially measured.

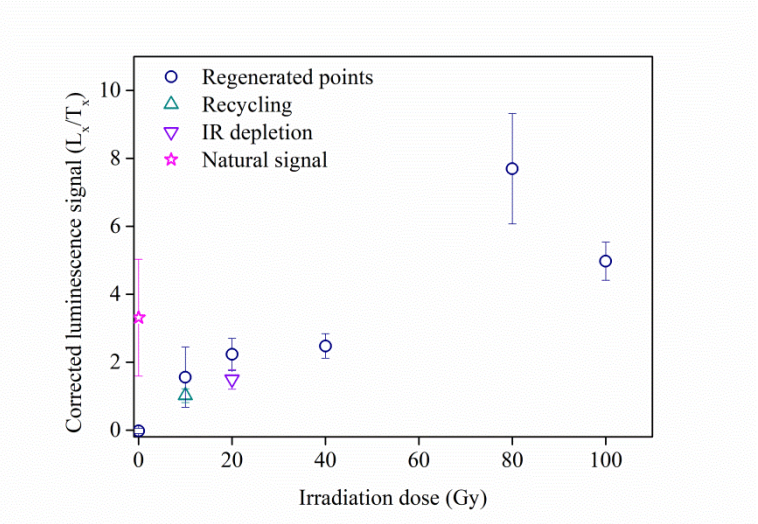

Figure 5.1 Representative sensitivity-corrected dose response curve. The sensitivity corrected natural signal is depicted as a star. Recycling and IR depletion points are represented as an upward triangle and inverse triangle, respectively.

We have further tested the behaviour of sample NZ3 63-90 μm quartz by performing a dose-recovery test. Three aliquots were bleached with blue diodes twice at room temperature for 100 s with a 10000 s pause in between the two stimulations. A dose of 100 Gy was then administered and measured as unknown, using the SAR protocol. One can ascertain that an increase in sensitivity occurs and sensitivity changes are not properly corrected by the measurement protocol, as observed from recycling tests. This results in an unsatisfactory recovered-to-given dose ratio.

Preusser et al. (2006) have attributed this poor OSL behaviour of quartz to the short sedimentary history of the grains, as it was reported that sensitisation of the OSL signal was achieved by repeated bleaching/irradiation cycles.

To test whether OSL properties of the samples investigated here can be improved by the application of different irradiation and stimulation steps, we have conducted a dose recovery test on sample NZ3 63-90 μm under the same conditions, except that the whole procedure was carried out subsequent to the application of three different treatments:

(i) the repetition of 5 bleach (blue diodes stimulation for 100 s at room temperature)/dose (100 Gy) cycles,

(ii) irradiating the sample with a dose of 100 Gy followed by heating to 500°C five times and

(iii) simply by repeating five times the heat treatment that consistied of a ramp heating to 500°C.

We have not observed an increase in sensitivity or an improvement in the results of the dose recovery test – in other words, a better behaviour of the material in the SAR protocol in accordance with the following treatment, namely (i) the application of repeated bleach/dose cycles. However, the sensitivity is increased by one order of magnitude following dosing and annealing, with the heat treatment accounting for most of the effect, as can be seen from the results of experiment (ii) where irradiations have not been carried out. Following the application of the annealing to 500°C, the behaviour of the OSL signals in the SAR protocol is improved, with satisfactory recycling and dose recovery tests results.

5.4.2 Luminescence properties – Polymineral fine grains

Equivalent doses

Unlike OSL signals of quartz, the IRSL signals of polymineral fine grains displayed a satisfactory behaviour in the SAR protocol. The values for the equivalent doses range from 64 ± 2 Gy to 92 ± 23 Gy in the case of $pIRIR_{225}$ protocol and from 83 ± 3 Gy to 120 ± 6 Gy in the case of $pIRIR_{290}$ protocol, respectively.

Residual signals

To quantify residual values, four fresh aliquots from each sample were exposed to window for 30 days to remove the natural signal and quantify the residual level. Residual doses measured using the $pIRIR_{225}$ protocol range from 3.3 ± 0.4 Gy to 3.7 ± 0.3 Gy, while the values obtained using the $pIRIR_{290}$ protocol are from 4.1 ± 0.6 Gy to 13.6 ± 2.5 Gy.

To check whether this is indeed the minimum residual level that can be achieved as function of exposure time, sets of five fresh aliquots of sample NZ5 were exposed to window light for different periods of time (from 0.5 h to 192 h). The results are shown in **Figure 5.4**. In the case of $pIRIR_{225}$ protocol, a constant residual dose of 3.7 ± 0.5 Gy is achieved after 48 h of exposure, while in the case of the $pIRIR_{290}$, signals' residual values reach a constant value of 9.8 ± 0.5 Gy only after a bleaching time of 96 h. These results are in line with the values obtained for the 30-day-experiment.

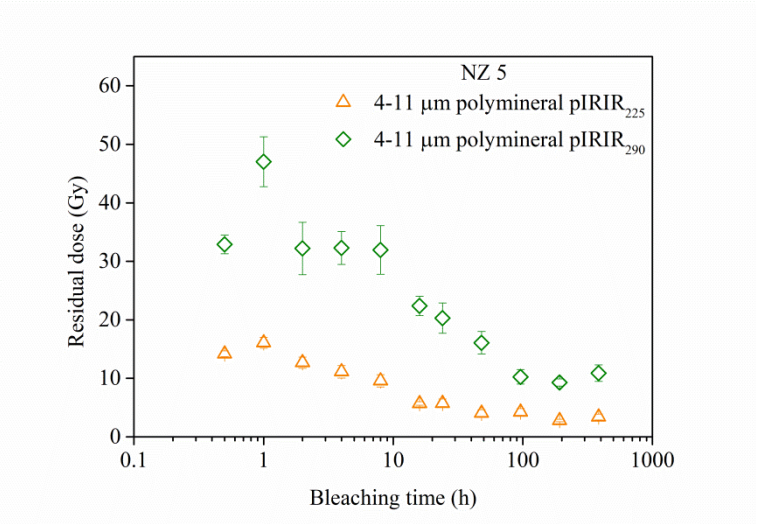

Figure 5.4 Residual doses measured using pIRIR225 (upward triangle) and pIRIR290 (diamond) after different bleaching times. The natural signal was bleached under natural conditions under window light. The shortest bleaching time was 0.5 h while the longest was 192 h. pIRIR, post-infrared–infrared protocol.

To investigate whether the residual signal is dose dependent, eight bleached aliquots of samples were irradiated with different beta doses of 400 Gy, 800 Gy and 1600 Gy and subsequently exposed to windowlight. After an exposure of 30 days, four aliquots from each sample were measured using $pIRIR_{225}$ protocol, whereas for the other four aliquots, the $pIRIR_{290}$ protocol was used. An increase of the residual dose with the size of the previously given dose can be observed in the case of both pIRIR protocols. The magnitude of the residuals range from 5.9 ± 0.7 Gy (for a dose of 400 Gy) to 8.9 ± 1 Gy (for a dose of 1600 Gy) in the case of $pIRIR_{225}$ and from 13.9 ± 1.2 Gy (for a dose of 400 Gy) to 18.5 ± 1.7 Gy (for a dose of 1600 Gy) in the case of $pIRIR_{290}$, respectively.

We compare the data obtained for 1600 Gy (8.9 ± 1 Gy for $pIRIR_{225}$ and 18.5 ± 1.7 Gy for $pIRIR_{290}$) to the values obtained in the bleaching experiment for the natural signals (corresponding to a measured equivalent dose of ≅60–120 Gy), namely average values on all samples of 3.5 ± 0.2 Gy for $pIRIR_{225}$ and 9.2 ± 2.0 Gy for $pIRIR_{290}$, respectively. We conclude that (i) different doses accrued by the mineral grain before the bleaching event should not result in dramatically different residual doses and (ii) performing bleaching experiments on natural samples instead of using a modern analogue should not result in an offset of more than a few Grays. Bleaching corrections should not cause significant inaccuracies unless very young samples are dated. However, it is advisable to measure a modern analogue for residual dose estimation, as well. Here, a modern sample was collected from a nearby site (latitude 44.014973° S, longitude 171.891569° E). Following the same

methodology, an equivalent dose of 7.5 ± 0.5 Gy was measured using $pIRIR_{225}$ protocol; on the other hand, using $pIRIR_{290}$ protocol, a dose of 22.8 ± 1.5 Gy was obtained. Based on the results of the laboratory experiments presented above, we consider these residual doses as maximum values. We have chosen to perform residual corrections using both laboratory obtained values, as well as by the modern analogue approach.

Dose recovery

Dose recovery ratios obtained for the $pIRIR_{225}$ protocol range from 0.97 ± 0.02 (NZ 2) to 1.03 ± 0.01 (NZ 5), while for $pIRIR_{290}$ they range from 1.02 ± 0.04 (NZ 2) to 1.09 ± 0.05 (NZ 3), suggesting that both $pIRIR_{225}$ and $pIRIR_{290}$ protocols can successfully recover the laboratory doses given.

Anomalous fading tests

The stability of the $pIRIR_{225}$ signal was checked by an anomalous fading test performed on three 4–11 μm polymineral fine grain aliquots of samples NZ 2, NZ 4 and NZ 5. The maximum time delay was 38 days (912 h). A fading rate <1%/decade was obtained for sample NZ 2 and NZ 5, while for sample NZ 4 a g-value of 2.28 ± 0.44%/decade was obtained. Therefore, the $pIRIR_{225}$ and $pIRIR_{290}$ ages presented in this study are not corrected for fading, except for sample NZ 4, for which a fading correction using the R Luminescence-package (**Dietze *et al.*, 2013**) according to **Huntley and Lamothe (2001)** method was carried out.

Luminescence ages

Only the ages obtained by residual dose correction using the modern analogue technique are represented as function of depth in **Figure 5.5**. The $pIRIR_{225}$-ages range from 14 ± 1 ka to 25 ± 2 ka; on the other hand, the $pIRIR_{290}$-ages are slightly higher than $pIRIR_{225}$-ages, but still in agreement within errors for all samples. The $pIRIR_{290}$-ages vary between 14 ± 1 ka and 29 ± 3 ka.

The pIRIR-ages increase down-section, except for an age reversal between the sample NZ 4 and NZ 5. The ages suggest that loess from this site was deposited during the last glacial maximum of the Otira glaciation that occurred during 18– 24 ka (**Alloway *et al.*, 2007**).

5.5 Summary and Conclusion

The difficulty of obtaining reliable luminescence chronologies for loess in New Zealand South Island is well known. In this context, the applicability of SAR-OSL protocol on quartz as well as the feldspar-SAR–based $pIRIR_{225}$ and $pIRIR_{290}$ protocols on polymineral fine grains was investigated on four loess samples collected from the

Southern Canterbury Plains. OSL signals displayed low sensitivity and significant sensitivity-change during the measurement cycles. While equivalent doses could not be securely obtained using quartz, the application of $pIRIR_{225}$ and $pIRIR_{290}$ methods were successful in achieving the following outcomes, namely: (i) dose recovery tests resulted in satisfactory results for both these protocols, results being consistent to unity at a 95% confidence level; (ii) fading rates of $pIRIR_{225}$ signals were generally negligible, with measured values of less than 1%; (iii) although $pIRIR_{290}$ signals are more difficult to bleach than $pIRIR_{225}$ signals, constant residual values of ≅4 and ≅10 Gy were achieved after exposure under window light exposure for 48 h in the case of $pIRIR_{225}$ and 96 h in the case of $pIRIR_{290}$ signals, respectively; and (iv) a dependence of the residual on the previous given dose was observed; however, for a dose as large as 1600 Gy, the residuals obtained for the two methods are ≅9 and ≅19 Gy, respectively. Thus, the equivalent dose of the sample used in the bleaching experiment should not have a significant effect when the residual dose is determined by laboratory experiments. The ages obtained by the application of the two pIRIR protocols are generally in agreement, with values ranging from 14 ± 1 ka to 29 ± 3 ka, suggesting that loess from the investigated site was deposited during the last glacial maximum.

6. Summary and conclusion

Optically stimulated luminescence (OSL) dating brought important contributions to Quaternary chronological research especially since the development of the single aliquot regenerative (SAR) equivalent dose measurement procedure that allowed improving the precision of the dating results on sediments from various environments worldwide. Since quartz and feldspars are the most common minerals dating protocols based on their luminescence properties were developed. When quartz is chosen as the preferred dosimeter, SAR-OSL protocol is used. Contrary to quartz, feldspars are known to suffer from anomalous fading and thus the development during the last decade of protocols that are able to select signals that are not prone to fading significantly increased the popularity of using these minerals in luminescence dating studies. At the moment the most used protocol for feldspars dating is the post infrared-infrared stimulated luminescence (pIR-IRSL) protocol with an IR stimulation at 50 ^{0}C followed by another IR stimulation at higher temperature ($pIR_{50}IR_{T>50}$), during which the signal of interest is recorded. The most common used temperatures of stimulation are 225 ^{0}C and 290 ^{0}C and the measurement protocols are generically known as $pIRIR_{225}$ and $pIRIR_{290}$, respectively. In the framework of this PhD project the applicability of SAR-OSL, $pIRIR_{225}$ and $pIRIR_{290}$ protocols on quartz and polymineral fine grains extracted from loess from three continents, namely Europe, Asia and Oceania, was tested and the results were critically evaluated.

The first loess-paleosol sequence investigated in the present dissertation was Batajnica master section located in SE Europe where 5 loess-paleosol alternations are exposed, that were well documented in terms of magnetic susceptibility variations and this proxy was orbitally tuned to major episodes of climate change. For OSL dating, fine (4-11 μm) and coarse (63-90 μm) quartz as well as polymineral fine grains were extracted from 18 samples. Optically stimulated luminescence dating was applied by using SAR-OSL protocol on fine and coarse quartz while $pIRIR_{225}$ and $pIRIR_{290}$ protocols were used for polymineral fine grains equivalent dose determination. Because some samples were collected from the major loess-paleosol transitions that can be confidently assigned to transitions of marine isotope stages based on the orbitally tuned variations of the magnetic susceptibility proxy, expected equivalent doses were determined based on the expected ages. The luminescence characteristics of quartz, both fine and coarse fractions, were shown to exhibit a good behaviour in the SAR protocol, however the equivalent doses and ages underestimated the expected ages for samples collected below the S1 paleosoil, corresponding to marine isotope stage (MIS 5). Using polymineral fine grains

increase values of 490±21 Gy for $pIRIR_{290}$ protocol and 377±19 Gy in the case of $pIRIR_{225}$ protocol were obtained for a sample collected below S1 paleosol. In order to check the reliability of the equivalent doses obtained different tests were assessed for pIRIR protocols. The results showed that the magnitude of the test dose does not influence the equivalent dose. Moreover, residual doses were determined using both laboratory bleaching as well by using the modern analogue approach. Fading tests were carried out and the results lead us to conclude that there is likely no detectable fading. Further, the results of the dose recovery test showed good performance of the $pIRIR_{225}$ protocol for doses up to ~300 Gy while for the $pIRIR_{290}$ protocol the dose recovery ratio showed a systematically overestimation of the given laboratory dose for the entire dose range investigated in this study, namely up to 450 Gy. Finally, for assessing the dose interval for which each protocol provides reliable luminescence ages, natural and laboratory dose response curves (DRCs) were compared. The results showed that in the case of fine and coarse quartz, both curves overlap up to ~150 Gy and ~250 Gy, respectively. For $pIRIR_{225}$ protocol, an apparent overlap of the natural and laboratory growth curves up to at least ~500 Gy is observed while in the case of $pIRIR_{290}$ protocol, natural and laboratory DRCs are consistent for doses up to ~400 Gy beyond which the natural signals overestimate the laboratory signals.

Another loess profile of interest where the applicability of the aforementioned three protocols was evaluated, was a loess-paleosol deposit from southeastern China. The three sets of luminescence ages are in agreement up to ~70 ka, confirming that the ages obtained in this range are reliable and showing that the Xiashu loess was accumulated during the last Glaciation. Fine quartz SAR-OSL ages obtained for samples >70 ka are considered underestimated based on our previous experience with dating loess worldwide while polymineral fine grains pIRIR ages are interpreted as overestimates based on the results of the laboratory tests described below. Luminescence characteristics of quartz were evaluated by applying the SAR-OSL protocol on fine quartz while the luminescence properties of polymineral fine grains were assessed by using $pIRIR_{225}$ and $pIRIR_{290}$ protocols. The laboratory intrinsic test results suggested that SAR-OSL protocol is suitable for equivalent dose determination on fine quartz. In order to check if the pIRIR protocols can accurately measure a known laboratory given dose, dose recovery tests were performed. The results showed that $pIRIR_{225}$ protocol can successfully recover known doses up to ~ 300 Gy while for larger doses (>400 Gy) the measured doses start to overestimate the given dose. On the other hand, dose recovery results that were performed using $pIRIR_{290}$ protocol showed that the dose recovered by the protocol overestimates the given dose for the entire dose range investigated with a more severe overestimation

found for doses larger than 400 Gy. Further, fading tests was performed and the results confirmed our previous finds on Batajnica samples, namely that the fading rates measured using short-term standard fading measurements cannot be accurately determined and that there is likely not significant fading.

The last loess deposit investigated in this dissertation is localised in South Island of New Zealand. Due to the limited number of dating studies, a robust chronological framework for the South Island was not yet established and previous studies reported that quartz in this region is not suitable for luminescence dating. As such, we have conducted a detailed investigation on the luminescence properties of quartz as well as an evaluation of the suitability of the application of pIRIR protocols for dating four sedimentary samples from a deposit of loess in South Island by using polymineral fine grains. In order to assess the luminescence properties of quartz, the SAR-OSL protocol has been applied on fine (4-11 μm) quartz as well as on coarse (63-90, 90-125, 125-180 and 180-250 μm) quartz fractions. The results obtained on quartz showed that a very weak fast component is present in both natural and regenerative signals and a dose response curve could not be properly constructed. Moreover, sensitivity changes during repeated SAR cycle were observed. Therefore, $pIRIR_{225}$ and $pIRIR_{290}$ protocols were applied on polymineral fine grains which showed a satisfactory behaviour in the SAR procedure. Both pIRIR protocols can successfully measure given laboratory doses. Fading rates were insignificant here as well, therefore the ages were not corrected for fading. The residual dose measurements showed a dependency of the residual dose with the previous given dose. However, our bleaching experiment showed that for $pIRIR_{225}$ protocol a constant residual dose is achieved after 48 h exposure to sunlight while in the case of $pIRIR_{290}$ protocol the constant level is obtained after 96 h exposure. The luminescence ages suggested that the investigated site was deposited during the last glacial maximum.

Since pIRIR protocols have been applied on polymineral fine grains from three different continents, a significant amount of data that increases our understanding on the behaviour of these signals was obtained. It is well known that feldspars are more difficult to bleach than quartz and therefore residual dose measurements should be performed prior to age calculation. In order to accomplish this, several bleaching experiments have been carried out on samples investigated in this thesis such as: investigating the dependency of the residual as function of the exposure time to sunlight (form 0.5 h to 30 days), or the investigation of the dependency of the residual dose on the equivalent dose magnitude, as well as on the magnitude of various large laboratory given doses (up to 800 Gy). Our results

showed that $pIRIR_{290}$ signal is more slowly bleached than $pIRIR_{225}$ and the residual doses measured using $pIRIR_{290}$ protocol are larger than those measured with $pIRIR_{225}$ protocol. Assuming that the residual dose originates from an unbleachable component that is not dose dependent and the values measured in young samples are actually the result of insufficient exposure to light, a time which is characteristic to all samples investigated in a sedimentary context, if the bleaching time is maintained to a fixed period during solar simulator experiments on different samples, then a linear dependency is expected between the equivalent dose of the investigated samples and the measured residual dose values. Therefore, a minimum residual dose corresponding to the unbleachable part of the signal can be determined by extrapolating measured residual dose values to an equivalent dose equal to 0 Gy (De = 0 Gy). In the absence of information from modern analogues, which is a common scenario in many dating contexts this is the most reasonable value to be subtracted from the measured equivalent dose when age calculation is performed.

The results of the fading measurements performed on polymineral fine grains extracted from Serbia, China and New Zealand loess which were carried out on quartz as well as a standard, since it is unanimously accepted that quartz does not suffer from fading, have demonstrated that fading is insignificant for $pIRIR_{225}$ signals.

Another controversial issue of the pIRIR protocols applicability is the dose recovery test performance. The results obtained in the framework of this thesis showed that the $pIRIR_{225}$ protocol can successfully recover known doses up to ~300-400 Gy while $pIRIR_{290}$ protocols tend to result in doses that slightly overestimate the given dose in the entire dose rage, with the overestimation being more significant for larger doses.

While the applicability of the SAR-OSL protocol on New Zealand quartz was hampered by the poor-luminescence behaviour of the material the application of the SAR-OSL protocol on quartz has resulted in obtaining robust chronologies for quartz extracted from Serbian and Chinese loess for ages up to about 70ka. Based on the natural and laboratory dose response curves constructed for Batajnica samples we conclude that fine and coarse quartz luminescence ages can be accurately measured up to doses of ~150 Gy and ~250 Gy, respectively.

Feldspars were shown to be able to extend the datable dose range by our study up to 400 Gy. However, our results showed that $pIRIR_{225}$ and $pIRIR_{290}$ overestimate the expected ages for samples with equivalent doses > ~ 400 Gy and therefore these ages obtained in this dose range should be interpreted with caution

in the absence of independent age control. Overall, keeping in mind the above-mentioned limitations, the results presented in this thesis have shown that pIRIR protocols can be applied successfully on polymineral fine grains extracted from loess deposits over three continents for extending the age range available by quartz dating.

References

Aitken, M.J., 1998. An Introduction to Optical Dating. 267. Oxford University Press, London.

Adamiec, G. 2000. Variations in luminescence properties of single quartz grains and their consequences for equivalent dose estimation. Radiation Measurements 32, 427-432.

Alloway, B.V., Lowe, D.J., Barrell, D.J.A., Newnham, R.M., Almond, P.C., Augustinus, P.C., Bertler, N.A.N., Carter, L., Litchfield, N.J., McGlone, M.S., Shulmeister, J., Vandergoes, M., Williams, P., NZ-INTIMATE Members., 2007. Towards a climate event stratigraphy for New Zealand over the past 30 000 years (NZ-INTIMATE project). Journal of Quaternary Science 22, 9-35.

Anechitei-Deacu, V., Timar-Gabor, A., Fitzsimmons, K.E., Veres, D., Ulrich, H. 2014. Multi-method luminescence investigations on quartz grains of different sizes extracted from a loess section in Southeast Romania interbedding the Campanian Ignimbrite ash layer. Geochronometria 41, 1-14.

Anechitei-Deacu, V., Timar-Gabor, A., Constantin, D., Trandafir-Antohi, O., del Valle, L., Fornos, J.-J., Gomez-Pujol, L., Wintle, A.G., 2018. Assesing the maximum limit of SAR-OSL dating using quartz of different grain sizes. Geochronometria 45, 146-159.

An, Z.S., Kukla, G.J., Porter, S.C., Xiao, J., 1991. Magnetic susceptibility evidence of monsoon variation on the Loess Plateau of central China during the last 130,000 years. Quaternary Research 36, 29–36.

Avram, A., Constantin, D., Veres, D., Kelemen, S., Obreht, I., Hambach, U., Marković, S.B., Timar-Gabor, A., 2020. Testing polymineral post-IR IRSL and quartz SAR-OSL protocols on Middle to Late Pleistocene loess at Batajnica, Serbia. Boreas 49, 615-633.

Bailey, R.M. 2001. Towards a general kinetic model for optically and thermally stimulated luminescence of quartz. Radiation Measurements 33, 17-45.

Bailey, R.M., 2002. Simulations of Variability in the Luminescence Characteristics of Natural Quartz and its Implications for Estimates of Absorbed Dose. Radiation Protection Dosimetry 100, 33-38.

Bailey, R.M., 2004. Paper I—simulation of dose absorption in quartz over geological timescales and its implications for the precision and accuracy of optical dating. Radiation Measurements 38, 299-310.

Baril, M.R., 2002. Spectral Investigations of luminescence in feldspars. Simon Fraser University, phD thesis.

Basarin, B., Buggle, B., Hambach, U., Markovic, S.B., O'Hara-Dhand, K., Kovacevic, A., Stevens, T., Guo, Z.T., Lukic, T., 2014. Time-scale and astronomical forcing of Serbian loess-paleosol sequences. Global and Planetary Change 122, 89-106.

Bøtter-Jensen, L., McKeever, A.W.S., Wintle, A.G. 2003. Optically Stimulated Luminescence Dosimetry. Elsevier Science B.V: Amsterdam, Netherlands, pp. 15-60, 119-234.

Bösken, J., Klasen, N., Zeeden, C., Obreht, I., Marković, S. B., Hambach, U., Lehmkuhl, F., 2017. New luminescence-based geochronology framing the last two glacial cycles at the southern limit of European Pleistocene loess in Stalać (Serbia). Geochronometria 44, 150–161

Buylaert, J.P., Vandenberghe, D., Murray, A.S., Huot, S., De Corte, F., Van den Haute, P. 2007. Luminescence dating of old (>70 ka) Chinese loess: A comparison of single aliquot OSL and IRSL techniques. Quaternary Geochronology 10, 75–80.

Buylaert, J.P., Murray, A.S., Vandenberghe, D., Vriend, M., De Corte F., Van den haute, P., 2008. Optical dating of Chinese loess using sand-sized quartz: Establishing a time frame for Late Pleistocene climate changes in the western part of the Chinese Loess Plateau. Quaternary Geochronology 3, 99-113.

Buylaert, J.-P., Murray, A.S., Thomsen, K. J., 2009. Testing the potential of an elevated temperature IRSL signal from K-feldspar. Radiation Measurements 44, 560–565.

Buylaert, J.-P., Huot, S., Murray, A.S., Van Den Haute, P. 2011a. Infrared stimulated luminescence dating of an Eemian (MIS 5e) site in Denmark using K-feldspar. Boreas 40, 46–56.

Buylaert, J.-P., Thiel, C., Murray, A.S., Vandemberghe, D.A.G., Yi, S., Lu, H. 2011b. IRSL and post-IR IRSL residual doses recorded in modern dust samples from the Chinese loess plateau. Geochronometria 38, 432–440.

Buylaert, J.-P., Jain, M., Murray, A.S., Thomsen, K.J., Thiel, C., Sohbati, R. 2012. A robust feldspar luminescence dating method for Middle and Late Pleistocene sediments. Boreas 41, 435–451.

Buggle, B., Hambach, U., Glaser, B., Gerasimenko, N., Marković, S., Glaser, I., Zöller, L., 2009. Stratigraphy, and spatial and temporal paleoclimatic trends in Southeastern/Eastern European loess–paleosol sequences. Quaternary International 196, 86-106.

Buggle, B., Hambach, U., Kehl, M., Marković, S.B., Zöller, L., Glaser, B., 2013. The progressive evolution of a continental climate in southeast-central European lowlands during the Middle Pleistocene recorded in loess paleosol sequences. Geology 41, 771-774.

Colarossi, D., Duller, G.A.T., Roberts, H.M., 2018. Exploring the behaviour of luminescence signals from feldspars: Implications for the single aliquot regenerative dose protocol. Radiation Measurements 109, 35-44.

Chapot, M.S., Roberts, H.M., Duller, G.A.T., Lai, Z.P. 2012. A comparison of natural and laboratory-generated dose response curves for quartz optically

stimulated luminescence signals from Chinese Loess. Radiation Measurements 47, 1045–1052.

Constantin, D., Timar-Gabor, A., Veres, D., Begy, R., Cosma, C. 2012. SAR-OSL dating of different grain-size quartz from a sedimentary section in southern Romania interbedding the Campanian Ignimbrite/Y5 ash layer. Quaternary Geochronology 10, 81–86.

Constantin, D., Begy, R., Vasiliniuc, S., Panaiotu, C., Necula, C., Codrea, V., Timar-Gabor, A. 2014. High-resolution OSL dating of the Costinești section (Dobrogea, SE Romania) using fine and coarse quartz. Quaternary International 334, 20–29.

Dietze, M., Kreutzer, S., Fuchs, M.C., Burrow, C., Fischer, M., Schmidt, C., 2013. A practical guide to the R package luminescence. Ancient TL 31, 11-18.

Duller, G.A.T., Bøtter-Jensen, L., Murray, A.S. 2000. Optical dating of single sand-sized grains of quartz: sources of variability. - Radiation Measurements 32, 453-457.

Duller, G.A.T. 2004. Luminescence dating of Quaternary sediments: recent advances. Journal of Quaternary Science 19, 183-192.

Groza-Săcaciu, S.M., Panaiotu, C., Timar-Gabor, A. 2020. Single aliquot regeneration (SAR) optically stimulated luminescence dating protocols using different grain-sizes of quartz: revisiting the Chronology of Mircea Vodă loess-paleosol master section (Romania). Methods and Protocols 3, 19.

Han, L., Hao, Q., Qiao, Y., Wang, L., Peng, S., Li, N., Gao, X., Fu, Y., Xu, B., Gu, Z., 2019. Geochemical evidence for provenance diversity of loess in southern China and its implications for glacial aridification of the northern subtropical region. Quaternary Science Reviews 212, 149-163.

Hao, Q., Guo, Z., Qiao, Y., Xu, B., Oldfield, F., 2010. Geochemical evidence for the provenance of middle Pleistocene loess deposits in southern China. Quaternary Science Review 29, 3317–3326.

Hao, Q., Wang, L., Oldfield, F., Peng, S., Qin, L., Song, Y., Xu, B., Qiao, Y., Bloemendal, J., Guo, Z., 2012. Delayed build-up of Arctic ice sheets during 400,000-year minima in insolation variability. Nature 490, 393–396.

Hansen, V., Murray, A., Buylaert, J.-P., Yeo, E.-Y., Thomsen, K., 2015. A new irradiated quartz for beta source calibration. Radiation Measurements 81, 123–127.

Huntley, D.J., Lamothe, M., 2001. Ubiquity of anomalous fading in K-feldspars and the measurement and correction for it in optical dating. Canadian Journal of Earth Sciences 38, 1093-1106.

Huntley, D.J., Lian, O.B., 2006. Some observations on tunnelling of trapped electrons in feldspars and their implications for optical dating. Quaternary Science Reviews 25, 2503-2512.

Jain, M., Ankjaergaard K., 2011. Towards a non-fading signal in feldspar: Insight into charge transport and tunnelling from time-resolved optically stimulated luminescence. Radiation Measurements 46, 292-309.

Jiang, Q., Hao, Q., Peng, S., Qiao, Y., 2020. Grain-size evidence for the transport pathway of the Xiashu loess in northern subtropical China and its linkage fluvial systems. Aeolian Research 46, 100613.

Kreutzer, S., Fuchs, M., Meszner, S., Faust, D. 2012. OSL chronostratigraphy of a loess palaeosol sequence in Saxony/Germany using quartz of different grain sizes. Quaternary Geochronology 10, 102-109.

Lapp, T., Kook, M., Murray, A. S., Thomsen, K. J., Buylaert, J.-P., Jain, M., 2015. A new luminescence detection and stimulation head for the Risø TL/OSL reader. Radiation Measurements 81, 178–184.

Lisiecki, L.E., Raymo, M.E., 2005. A Pliocene-Pleistocene stack of 57 globally distributed benthic δ18O records. Paleoceanography 20, PA1003.

Li, Y., Tsukamoto, S., Frechen, M., Gabriel, G., 2018. Timing of fluvial sedimentation in the Upper Rhine Graben since the Middle Pleistocene: constraints from quartz and feldspars luminescence dating. Boreas 47, 256-270.

Li, X., Han, Z., Lu, H., Chen, Y., Li, Y., Yuan, X., Zhou, Y., Jiang, M., Lv, C., 2018. Onset of Xiashu loess deposition in southern China by 0.9 Ma and its implications for regional aridification. Science China Earth Sciences 61, 256–269.

Liu, T.S., 1985. Loess and the Environment. China Ocean Press, Beijing, pp 65-251.

Lu, Y.C., Zhao, H., Yin, G.M., Chen, J., Zhang, J.Z., 1999. Luminescence dating of loess–paleosol sequences in the past about 100 ka in North China. Bulletin of the National Museum of Japanese History 81, 209–220.

Lu, Y.C., Wang, X.L., Wintle, A.G., 2007. A new OSL chronology for dust accumulation in the last 130,000 yr for the Chinese Loess Plateau. Quaternary Research 67, 152-160.

Lowick, S.E., Preusser, F., Wintle, A.G. 2010. Investigating quartz optically stimulated luminescence dose response curves at high doses. Radiation Measurements 45, 975–984.

Lai, Z.P., 2010. Chronology and the upper dating limit for loess samples from Luochuan section in the Chinese Loess Plateau using quartz OSL SAR protocol. Jpurnal of Asian Earth Sciences 37, 176-185.

Marković, S.B., Hambach, U., Catto, N., Jovanovic, M., Buggle, B., Machalett, B., Zöller, L., Glaser, B., Frechen, M., 2009. Middle and Late Pleistocene loess sequences at Batajnica, Vojvodina, Serbia. Quaternary International 198, 255-266.

Marković, S.B., Stevens., T., Kukla, G.J., Hambach, U., Fitzsimmons, K., Gibbard, P., Buggle, B., Zech, M., Guo, Z., Hao, Q., Wu, H., O'Hara-Dhand, K., Smalley, I., Újvári, G., Sümegi, P., Timar-Gabor, A., Veres, D., Sirocko, F., Vasiljevic, D., Svirčev, Z. 2015. Danube loess stratigraphy – Towards a pan-European loess stratigraphic model. Earth-Science Reviews 148, 228-258.

Muhs, D.R. 2007. Loess deposits, origins, and properties. In: Elias, S. (Ed.), The encyclopedia of Quaternary sciences. Elsevier, Amsterdam, Netherlands, 1405–1418.

Murray, A.S. 1996. Developments in optically stimulated luminescence and photo-transferred thermoluminescence dating of young sediments: application to a 2000-years of flood deposits. Geochimica et Cosmochimica Acta 60, 565–576.

Murray, A.S., Wintle, A.G. 2000. Luminescence dating of quartz using an improved single aliquot regenerative-dose protocol. Radiation Measurements. 32, 57–73.

Murray, A.S., Olley, J.M. 2002. Precision and accuracy in the optically stimulated luminescence dating of sedimentary quartz: a status review. Geochronometria 21, 1-16.

Murray, A.S., Wintle, A.G. 2003. The single aliquot regenerative dose protocol: potential for improvements in reliability. Radiation Measurements 37, 377-381.

Murray, A.S., Svendsen, J.I., Mangerund, J.I., Astakhov, V.I. 2007. Testing the accuracy of quartz OSL dating using a known-age Eemian site on the river Sula, northern Russia. Quaternary Geochronology 2, 102–109.

Murray, A.S., Thomsen, K.J., Masuda, N., Buylaert, J.P., Jain, M., 2012. Identifying well-bleached quartz using the different bleaching rates of quartz and feldspar luminescence signals. Radiation Measurements 47, 688–695.

Murray, A.S., Schmidt, E.D., Stevens, T., Buylaert, J.-P., Marković, S.B., Tsukamoto, S., Frechen, M., 2014. Dating Middle Pleistocene loess from Stari Slankamen (Vojvodina, Serbia) – Limitations imposed by the saturation behaviour of an elevated temperature IRSL signal. Catena 117, 34–42.

Moska, P., Murray, A.S. 2006. Stability of the quartz fast-component in insensitive samples. Radiation Measurements 41, 878-885.

Necula, C., Dimofte, D., Panaiotu, C. 2015. Rock magnetism of a loess-palaeosol sequence from western Black Sea shore (Romania). Geophysical Journal International 202, 1733-1748.

Preusser, F., Ramseyer, K., Schlüchter, C. 2006. Characterisation of low OSL intensity quartz from the New Zealand Alps. Radiation Measurements 41, 871-877.

Pagonis, V., Chen, R., Wintle, A.G., 2007. Modelling thermal transfer in optically stimulated luminescence of quartz. Journal of Physics D: Applied Physics 40, 998.

Pagonis, V., Wintle, A.G., Chen, R., Wang, X.L., 2008. A theoretical model for a new dating protocol for quartz based on thermally transferred OSL (TT-OSL). Radiation Measurements 43, 704-708.

Perić, Z., Lagerbäck Adolphi, E., Stevens, T., Újvári, G., Zeeden, C., Buylaert, J.P., Marković, S.B., Hambach, U., Fischer, P., Schmidt, C., Schulte, P., Huayu, L., Shuangwen, Y., Lehmkuhl, F., Obreht, I., Veres, D., Thiel, C., Frechen, M., Jain, M., Vött, A., Zöller, L., Gavrilov, M.B., 2019. Quartz OSL dating of late quaternary Chinese and Serbian loess: A cross Eurasian comparison of dust mass accumulation rates. Quaternary International 502, 30-44.

Pye, K. 1987. Aeolian Dust and Dust Deposits. Academic Press: San Diego, CA, USA, 334.

Pye, K. 1995. The nature, origin and accumulation of loess. Quaternary Science Reviews 14, 653–657.

Poolton, N.R.J., Wallinga, J., Murray A.S., Bulur, E., Bøtter-Jensen L., 2002a. Electrons in feldspar I: on the wavefunction of electrons trapped at simple lattice defects. Physics and Chemistry of Minerals 29, 210-216.

Poolton, N.R.J., Ozanyan K.B., Wallinga, J., Murray A.S., Bøtter-Jensen L., 2002b. Electrons in feldspar II: a consideration of the influence of conduction band-tail states on luminescence processes. Physics and Chemistry of Minerals 29, 217-225.

Qiao, Y.S., Guo, Z.T., Hao, Q.Z., Wu, W.X., Jiang, W.Y., Yuan, B.Y., Zhang, Z.S., Wei, J.J., Zhao, H., 2003. Loess-soil sequences in southern Anhui Province: magnetostratigraphy and paleoclimatic significance. Chinese Science Bulletin 48, 2088–2093.

Rhodes, E.J., Bronk-Ramsey, C., Outram, Z., Batt, C., Willis, L, Dockrill, S.J., Bond, J. 2003. Bayesian methods applied to the interpretation of multiple OSL dates: High precision sediment ages from Old Scatness Broch excavation, Shetland Island. Quaternary Science Reviews 22, 1231-1244.

Roberts, H., 2008. The development and application of luminescence dating to loess deposits: a perspective on the past, present and future. Boreas 37, 483–507.

Sohbati, R., Borella, J., Murray, A., Quigley, M., Buylaert, J.-P., 2016. Optical dating of loessic hillslope sediments constrains timing of prehistoric rockfalls, Christchurch, New Zealand. Journal of Quaternary Science 31, 678-690.

Spooner, N.A., 1992. Optical dating: preliminary results on the anomalous fading of luminescence from feldspars. Quaternary Science Reviews 11, 139-145.

Spooner, N.A., 1994. The anomalous fading of infrared-stimulated luminescence from feldspars. Radiation Measurements 23, 625-632.

Stevens, T., Armitage, S.J., Lu, H., Thomas, D.S.G., 2006. Sedimentation and diagenesis of Chinese loess: implications for the preservation of continuous high-resolution climate records. Geology 34, 849-852.

Stevens, T., Markovic, S.B., Zech, M., Hambach, U., Sümegi, P. 2011. Dust deposition and climate in the Carpathian Basin over an independently dated last glacial-interglacial cycle. Quaternary Science Reviews 30, 662–681.

Stevens, T., Buylaert, J.-P., Thiel, C., Újvári, G., Yi, S., Murray, A. S., Frechen, M., Lu, H., 2018. Ice-volume-forced of the Chinese Loess Plateau global Quaternary stratotype site. Nature Communications 9, 983.

Thomsen, K.J., Murray, A.S., Jain, M., Bøtter-Jensen, L., 2008. Laboratory fading rates of various luminescence signals from feldspar-rich sediment extracts. Radiation Measurements 43, 1474-1486.

Timar, A., Vandenberghe, D., Panaiotu, C.G., Necula, C., Cosma, C., van den haute, P., 2010. Optical dating of Romanian loess usinf fine-grained quartz. Quaternary Geochronology 5, 143-148.

Timar-Gabor, A., Vandenberghe, D.A.G., Vasiliniuc, S., Panaiotu, C.E., Panaiotu, C.G., Dimofte, D., Cosma, C. 2011. Optical dating of Romanian loess: A comparison between silt sized and sand-sized quartz. Quaternary International 240, 62–70.

Timar-Gabor, A., Vasiliniuc, S., Vandenberghe, D.A.G., Cosma, C., Wintle, A.G. 2012. Investigations into the reliability of SAR-OSL equivalent doses obtained for quartz samples displaying dose response curves with more than one component. Radiation Measurements 47, 740–745.

Timar-Gabor, A., Wintle, A.G. 2013. On natural and laboratory generated dose response curves for quartz of different grain sizes from Romanian loess. Quaternary Geochronology 18, 34–40.

Timar-Gabor, A., Constantin, D., Marković, S.B., Jain, M. 2015a. Extending the area of investigation of fine versus coarse quartz optical ages from the Lower Danube to the Carpathian Basin. Quaternary International 388, 168–176.

Timar-Gabor, A., Constantin, D., Buylaert, J.P., Jain, M., Murray, A.S., Wintle, A.G. 2015b. Fundamental investigations of natural and laboratory generated SAR dose response curves for quartz OSL in the high dose range. Radiation Measurements 81, 150–156.

Timar-Gabor, A., Buylaert, J.-P., Guralnik, B., Trandafir-Antohi, O., Constantin, D., Anechitei-Deacu, V., Jain, M., Murray, A.S., Porat, N., Hao, Q. 2017. On the importance of grain size in luminescence dating using quartz. Radiation Measurements 106, 464–471.

Tecsa, V., Gerasimenko, N., Veres, D., Hambach, U., Lehmkuhl, F., Schulte, P., Timar-Gabor, A., 2020a. Revisiting the chronostratighraphy of Late Pleistocene loess-paleosol sequences in southwestern Ukraine: OSL dating of Kurotne section. Quaternary International 542, 65-79.

Tecsa, V., Mason, J.A., Johnson, W.C., Miao, X., Constantin, D., Radu, S., Magdas, D.A., Veres, D., Marković, Timar-Gabor, A., 2020b. Latest Pleistocene to Holocene loess in the central Great Plains: Optically stimulated luminescence dating and multi-proxy analysis of the Enders loess section (Nebraska, USA). Quaternary Science Reviews 229, 106130.

Thiel, C., Buylaert, J.-P., Murray, A., Terhorst, B., Hofer, I., Tsukamoto, S., Frechen, M., 2011a. Luminescence dating of the Stratzing loess profile (Austria) – Testing the potential of an elevated temperature post-IR IRSL protocol. Quaternary International 234, 23–31.

Thiel, C., Buylaert, J.-P., Murray, A.S., Tsukamoto, S., 2011b. On the applicability of post-IR IRSL dating to Japanese loess. Geochronometria 38, 369-378.

Thiel, C., Buylaert, J.-P., Murray, A.S., Elmejdoub, N., Jedoui, Y.,2012. A comparison of TT-OSL and post-IR IRSL dating of coastal deposits on Cap Bon peninsula, north-eastern Tunisia. Quaternary International 10, 209–217.

Vasiliniuc, Ș., Vandenberghe, D.A.G., Timar-Gabor, A., Panaiotu, C., Cosma, C., 2012. Testing the potential of elevated temperature post-IR IRSL signals for dating Romanian loess. Quaternary Geochronology 10, 75-80.

Vereș, D., Lane, C.S., Timar-Gabor, A., Hambach, U., Constantin, D., Szakács, Fülling, A., Onac, B.P. 2013. The Campanian IgnimbriteY5 tephra layer – a regional stratigraphic marker for Isotope Stage 3 deposits in the Lower Danube region, Romania. Quaternary International 293, 22-33.

Veres, D., Tecsa, V., Gerasimenko, N., Zeeden, C., Hambach, U., Timar-Gabor, A., 2018. Short-term soil formation events in last glacial east European loess, evidence from multi-method luminescence dating. Quaternary Science Reviews 200, 34-51.

Wang, X., Lu, H., Zhang, H., Wu, J., Hou, X., Fu, Y., Geng, J., 2018. Distribution, provenance, and onset of the Xiashu Loess in Southeast China with paleoclimatic implications. Journal of Asian Earth Sciences 155, 180–187.

Wallinga, J., Murray, A., Duller, G. 2000. Underestimation of equivalent dose in single-aliquot optical dating of feldspars caused by preheating. Radiation Measurements 32, 691–695.

Wacha, L., Frechen, M., 2011. The geochronology of the "Gorjanović loess section in Vukovar, Croatia.Quaternary International 240, 87–99.

Watanuki, T., Murray, A.S., Tsukamoto, S. 2003. A comparison of OSL ages derived from silt-sized quartz and polymineral grains from Chinese loess. Quaternary Science Reviews 22, 991-997.

Wintle, A.G., 1973. Anomalous fading of thermoluminescence in mineral samples. Nature 245, 143-144.

Wintle, A.G., Shackleton, N.J., Lautridou, J.P., 1984. Thermoluminescence dating of periods of loess deposition and soil formation in Normandy. Nature 310, 491-493.

Wintle, A.G., Murray, A.S. 2006. A review of quartz optically stimulated luminescence characteristics and their relevance in single-aliquot regeneration dating protocols. Radiation Measurements 41, 369–391.

Yi, S., Buylaert, J.-P., Murray, A.S., Lu, H., Thiel, C., Zeng, L., 2016. A detailed post-IR IRSL dating study of the Niuyangzigou loess site in northeastern China. Boreas 45, 644–657.

Yi, S., Li, X., Han, Z., Lu, H., Liu, J., Wu, J., 2018. High resolution luminescence chronology for Xiashu Loess deposits of Southeastern China. Journal of Asian Earth Sciences 155, 188-197.